MODIFICATION OF CHEMICAL AND MORPHOLOGICAL PROPERTIES OF LEAD-ACID BATTERY NEGATIVE ACTIVE MATERIAL

A Thesis Submitted to
the Graduate School of Engineering and Sciences of
İzmir Institute of Technology
in Partial Fulfillment of the Requirements for the Degree of

MASTER OF SCIENCE

in Chemical Engineering

by
Burak Muhammet KAMA

December 2014
İZMİR

We approve the thesis of **Burak Muhammet KAMA**

Examining Committee Members:

Prof. Dr. Mehmet POLAT
Department of Chemical Engineering, İzmir Institute of Technology

Prof. Dr. Fehime ÖZKAN
Department of Chemical Engineering, İzmir Institute of Technology

Prof. Dr. Nuran ELMACI
Department of Chemistry, İzmir Institute of Technology

18 December 2014

Prof. Dr. Mehmet POLAT
Supervisor, Department of Chemical Engineering,
İzmir Institute of Technology

Prof. Dr. Fehime ÖZKAN
Head of the Department of Chemical Engineering

Prof. Dr. Bilge KARAÇALI
Dean of the Graduate School of Engineering and Sciences

ACKNOWLEDGMENTS

I would like to express my sincere gratitude to my supervisor Prof. Dr. Mehmet POLAT and Prof. Dr. Hürriyet POLAT whose expertise, understanding, patience, motivation, enthusiasm, immense knowledge, guidance and encouragement added considerably to my graduate experience.

I am deeply indebted to Research Asst. Hasan ARSLANOĞLU of Fırat University whose encouragement, enthusiasm and grateful advices.

I would like to thank to the whole staff of Department of Chemical Engineering for their help and İnci Battery; Sevtap AKSOY, Sinan YILMAZ, Özgür ÇALIK, Hasan ÖZSÜMER.

In addition, a thank to Republic of Turkey Ministry of Science, Industry and Technology for its financial supporting with the project 'Mikro-hibrit Araçlar için Kurşun Asit Akü Negatif Malzemesinin Geliştirilmesi'

I would like to present my deepest thanks to my friends; Aybike Nil Olcay, Elif Suna SOP, Sema KIRKÖSE, Elif GÜNGÖRMÜŞ, Ahmet Uğur ÇİÇEK, Özgün DELİİSMAİL, Emrah KURT.

I express my warmest thanks to my love Fatma ERKUŞ for here endless love, patience and help.

This journey would not be possible without the support of my family. I am very grateful to my parents Nezihe KAMA and Muammer KAMA who supported me emotionally and financially during whole my life. I always knew that they believed in me and wanted the best for me. I hope to have honored them, especially my mother, she is the biggest supporter of my life.

ABSTRACT

MODIFICATION OF CHEMICAL AND MORPHOLOGICAL PROPERTIES OF LEAD-ACID BATTERY NEGATIVE ACTIVE MATERIAL

Lead-acid batteries which are indispensable equipment for motor vehicles are one of the most important electrochemical processes commercially thanks to their advantages, such as low cost and capability of providing high energy. The new generation cars which such as climates, smart screens, stronger engines etc., require the batteries which should have longer cycle life and higher cold-cranking ampere.

In this study, the aims were elucidating the exact working mechanism of lead-acid battery negative active material and improving the commercial lead-acid battery for micro-hybrid vehicles. For this purpose, experimental studies were separated to three parts. First one is the characterizing of negative electrode raw materials, leady oxide, lignosulfonate, carbon, barium sulfate. Second one is determination of rheological properties of negative paste in different cases. Third one is the preparation of pastes and then performance testes (reserve capacity, cold-cranking ampere and cycle life) of negative plates prepared from the pastes characterized in second part.

As a result of first part of studies, it was shown that the all of carbon materials and leady oxide suffer from agglomeration in lignosulfonate solutions prepared in different concentrations. In second part, the rheological properties of negative paste were determined in different preparation cases and shown that the amount of additives and preparation method has big effects.

Finally, the negative plates were prepared with two methods, wet and dry mixing. After that the plates were formed and then electrical tests were performed. Consequently, a battery which has better properties, physically and chemically, was obtained. However, this improvement was not enough due to the dispersion problems of carbon samples tested in this study.

ÖZET

KURŞUN ASİT AKÜ NEGATİF AKTİF MALZEMESİNİN KİMYASAL VE MORFOLOJİK ÖZELLİKLERİNİN MODİFİKASYONU

Motorlu taşıtların vazgeçilmez parçalarından biri olan kurşun asit aküler düşük maliyetleri ve yüksek enerji sağlama yetenekleri sayesinde ticari açıdan büyük öneme sahip elektrokimyasal proseslerden biridir. Daha güçlü motorlar, klimalar, akıllı ekranlar vs. ekipmanlar içeren yeni jenerasyon araçlar daha uzun çevrim ömrüne ve daha yüksek soğuk marş akımına sahip akülere ihtiyaç duymaktadır. Bu yüzden tüm dünyada birçok araştırmacı ve akü üreticileri otomotiv endüstrisi için bu elektrokimyasal prosesi geliştirmeye çalışıyor.

Bu çalışmada, ticari kurşun asit akülerin start-stop araçlar için geliştirilmesi ve negatif aktif malzemesinin çalışma mekanizmasının açıklanması amaçlanmıştır. Bu amaçla, deneysel çalışmalar üç parçaya ayrılmıştır. Birincisi, hammaddelerin, kurşun oksit, lignosülfonat, karbon ve baryum sülfat, karakterizasyonudur. İkinci kısımda ise negatif pastanın reolojik özellikleri belirlenmeye çalışılmıştır. Son olarak negatif pastalar hazırlanmış bunların karakterizasyonu ve elektriksel testleri gerçekleştirilmiştir.

İlk deneysel çalışmaların sonucu olarak, tüm karbon materyallerinin ve kurşun oksidin farklı lignosülfonat konsantrasyonlarında aglomerasyona maruz kaldığı görülmüştür. Buna ek olarak ikinci kısımda negatif pastanın reolojik özellikleri incelenmiş ve katkı miktarlarının ve hazırlanış şekillerinin büyük etkiye sahip olduğu gözlenmiştir.

Deneysel çalışmaların son kısmının sonucu olarak ise, negatif plakalar kuru ve yaş karışım olmak üzere iki farklı metotla hazırlanmıştır. Daha sonra plakalar formasyon işlemine alındı ve son olarak elektriksel testler gerçekleştirildi. Sonuç olarak, daha iyi fiziki ve kimyasal özelliklere sahip bir akü elde edilmiştir. Buna karşın, engellenemeyen karbon dispersiyon probleminden dolayı elde edilen akünün en iyisi olmadığı sonucuna varılmıştır.

TABLE OF CONTENTS

LIST OF FIGURES

LIST OF TABLES

CHAPTER 1

INTRODUCTION

1.1. Lead-Acid Batteries

Lead-acid batteries which consist of the positive and negative electrodes and sulfuric acid solution as an electrolyte are indispensable electrochemical power source to initiate an engine. In lead-acid battery technology, additives are used to improve the physical and chemical properties of negative active material. The range of additives is from 0.02 to 2.0% of leady oxide used for each one of them. These are;

Lignosulfonate (LS): After the Second World War synthetic materials used instead of the wooden separators to prevent short-circuits between positive and negative electrode. However, this change caused a decrease in the battery capacity at low temperatures. It was revealed that this problem was originated from absence of lignosulfonic acid which came from wooden separator to the electrolyte (Pavlov 2011f).

Carbon: Carbon materials, carbon black, graphite and activated carbon, are used in negative active material. The effect of carbon was summarized as the following (Moseley, Nelson, and Hollenkamp 2006).

i. Improving the overall conductivity of negative active material (NAM),
ii. Facilitating the formation of small isolated lead sulfate ($PbSO_4$) particles dissolving easily and retarding lead sulfate crystal growth
iii. Behaving like a electro-osmotic pump to help electrolyte diffusion to the inner NAM.

Barium sulfate ($BaSO_4$): $BaSO_4$ is used as a nucleation agent for $PbSO_4$ crystal formation and also guaranteed the uniform distribution of $PbSO_4$ on the active mass pore surface due to isomorphism between $PbSO_4$ and $BaSO_4$ (Pavlov 2011f).

Fiber glass: Fiber glass is used to prevent the negative active material from shedding and provide adherence of material to grid.

In the literature, there are a lot of researches to understand the effect of additives on the NAM. The studies about effect of LS show that it causes the formation of larger $PbSO_4$ crystals (Asai et al. 1981, Ekdunge and Simonsson 1989, Hirai et al. 2004).

Unlike this, some studies showed the opposite effect (Hampson et al. 1980, Ban et al. 2002). In addition, it was also found that LS suppresses charge-discharge process thereby it decreases cycle life of battery (Pavlov, Nikolov, and Rogachev 2010a). A lot of studies were also conducted with carbon materials as additives such as carbon black, graphite and activated carbons. However, the relationship between amount of carbon and type of carbon was not clearly demonstrated (Pavlov, Nikolov, and Rogachev 2011, Sawai et al. 2006, Boden et al. 2010). Many researches were also performed studies with $BaSO_4$. These studies are generally about its amount and its effect on the capacity and cycle life of a battery which is not clear also (Boden 1998, Vermesan et al. 2004).

In lead-acid batteries, there are a lot of failure mechanisms which lead to loss of performance, cycle life. These can be classified as follows (Ruetschi 2004).

- Anodic corrosion
- Positive active mass degradation
- Irreversible formation of $PbSO_4$ in the active mass
- Short-circuits
- Loss of water

Sulfation has been a major problem since invention of lead-acid batteries. When the negative plates are covered insoluble lead sulfates that can be attributed some specific cases which cause this situation. These are losing of capacity and voltage, increasing in internal resistance and decreasing in sulfuric acid concentration (Catherino, Feres, and Trinidad 2004).

Generally, battery is in partially discharged state, in other words not fully charged state. This is a supportive situation for $PbSO_4$ re-crystallization process to progress. That is, small $PbSO_4$ crystallites dissolve and precipitate onto the big $PbSO_4$ crystals. Hence, the sulfation of the negative plates continues and eventually $PbSO_4$ cover the all plates. However, on the positive plates, the discharge process occur hydrated zones of lead dioxide PbO_2 particles with a series of chemical reactions which hamper the occurring and growth of big $PbSO_4$ crystals. In addition to this, sulfation is blocked by small pore radii in PbO_2 active mass. Sulfation problem is shown only on negative plates (Pavlov 1992).

Therefore, there are studies going on all over the world to prevent the sulfation of negative active material. Using additives in lead-acid battery is one of the solutions of this problem but it is not adequate to solve this problem completely. They improve

the chemical and physical properties of battery when they are used in optimum amount. In addition to these common additives, a lot of researcher has suggested other additives such as BiO_2 and Ga_2O_3 (Saravanan, Ganesan, and Ambalavanan 2014).

As it is known, there are big innovations in automotive industry. The internal combustion engines are being improved to reduce emissions and fuel consumption. The micro-hybrid vehicles are one of these innovative produces. A micro-hybrid engine stops itself for a little time when the car stops, such as waiting times in traffic light, then it starts to work engine automatically when driver pushes the clutch pedal. This way, the engine saves the environment and reduces the fuel cost.

However, equipments such as radio, climate and headlamps etc., need the energy supplied by battery when the engine stops. It creates big problem for battery, because battery discharges and does not charge. Hence, lead sulfates forms on the negative electrode and then these convert to big and insoluble structures. Consequently, these lead sulfate structures cover all the negative plate and finally battery is failed.

The reasons caused the sulfation problem does not have an exact solution in lead-acid batteries. In literature, there are a lot of publications written to elucidate the mechanism of sulfation but they are not adequate. Moreover, the effect of additives both battery performance and sulfation cannot be explained clearly.

In this study, it was aimed to improve the commercial lead-acid battery for micro- hybrid (start-stop) vehicles and elucidate the exact working mechanism of lead-acid battery negative active material. For this purpose, experimental studies were separated in to two parts. First one is the characterizing of negative electrode raw materials, leady oxide, lignosulfonate, carbon, barium sulfate. Second one is determination of rheological properties of negative paste in different cases. Third one is the preparation of pastes and then performance testes (reserve capacity, cold-cranking ampere and cycle life) of negative plates prepared from the pastes characterized in second part.

CHAPTER 2

PRODUCTION AND PROPERTIES OF LEAD-ACID BATTERIES

2.1. Lead-Acid Batteries

Lead-acid batteries are rechargeable devices which convert chemical energy to electric energy to initiate an engine start. In internal-combustion-engined vehicles (ICEVs), an automotive battery provides a rapid pulse of high current for starting and while it is lower and continuous for other purposes. Even though in such service (float duty) the battery should not often be demanded to discharge it is also true for stationary batteries that is used for backup power in telecommunications and uninterruptible power supplies. However, traction batteries designed for electric vehicles (EVs), are frequently necessitated to experience the deep discharges and recharges over periods of a few hours (deep-discharge duty). Batteries used in hybrid electric vehicles (HEVs) and in remote area power supply systems (RAPS) are between above mentioned extreme cases. These are generally in intermediate state of charge, approximately 50% partial state-of-charge (PSoC) duty (Rand and Moseley 2009).

In all lead-acid battery types, lead dioxide, PbO_2, and spongy lead, Pb, are used as positive active material (PAM), and negative active material (NAM), respectively, and sulfuric acid, H_2SO_4, is the electrolyte.

The lead-acid batteries consist of six-two volt of cell connecting each other with current collectors. The separators are also placed between the each electrode to prevent short circuit.

The negative and positive electrodes have a high negative and positive equilibrium potential, respectively. By this potential difference, high electromotive force is generated. Furthermore, the positive electrode has high electron conductivity. This guarantees the participation of major part of PbO_2 during current generation. The other factor is that electrochemical process and structures forming in negative and positive electrode are reversible processes (Pavlov 2011b).

2.2. Working Principles of Lead-Acid Battery

When the lead –acid battery works, electrochemical processes take part in both electrodes. According the reactions, one mol Pb produces two electrons flowing to positive electrode. Hence, lead sulfate is occurred at both plates. The reaction that takes part in negative electrode is oxidation of lead and reduction of lead dioxide during discharge.

At positive electrode,

$$PbO_2 + HSO_4^- + 3H^+ + 2e^- \underset{\textbf{Charge}}{\overset{\textbf{Discharge}}{\rightleftharpoons}} PbSO_4 + 2H \qquad (2.1)$$

$E^0 = +1.690$ V

At negative electrode,

$$Pb + HSO_4^- \underset{\textbf{Charge}}{\overset{\textbf{Discharge}}{\rightleftharpoons}} PbSO_4 + H^+ + 2e^- \qquad (2.2)$$

$E^0 = -0.358$ V

where E^0 is the standard electrode potential for each reaction, i.e, the electrode is in a standard state.

The overall reaction is:

$$PbO_2 + Pb + 2H_2SO_4 \underset{\textbf{Charge}}{\overset{\textbf{Discharge}}{\rightleftharpoons}} PbSO_4 + 2H_2O \qquad (2.3)$$

$V^0 = +2.048$V

where $V^0$is the standard cell voltage. According the above electrochemical reactions, the electrons generated at the negative electrode flow the positive electrode through the conductor. It cause to loss of electric energy from cell to an external consumer. Unlike this, charge process occurs when there is external power source. The electrons produced at positive electrode flow from positive electrode to negative electrode so that lead sulfate is reduced to lead. Thanks to this reverse process, battery re-charged with electric energy. The electric energy that is lost per unit charge is the cell voltage. It is presumed that electric current and electron flows are opposite way.

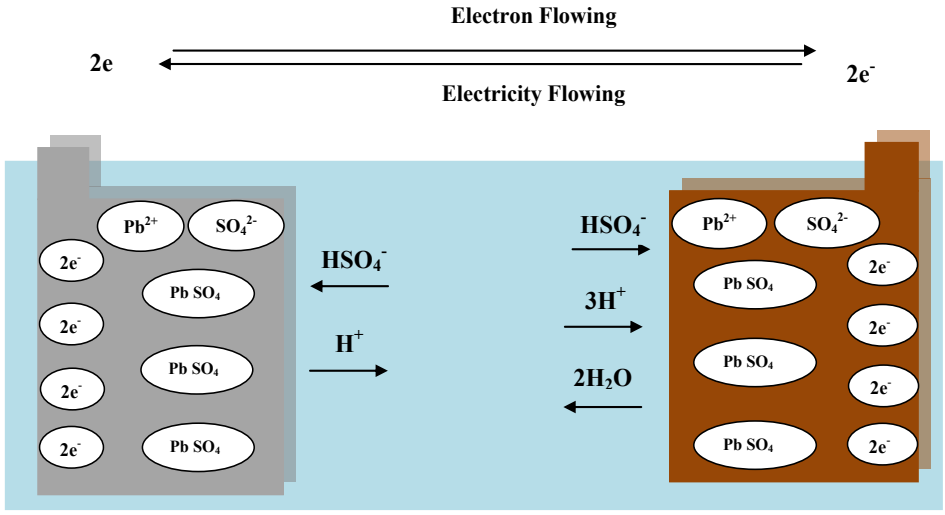

Figure 2.1. A schematic representation for lead-acid battery working principle

As it seen that HSO_4^- ions relocate to the negative electrode to react with the lead to form H^+ ions and lead sulfate ($PbSO_4$) which is extremely non-conductive component. When both plates are discharged the surface of them with lead sulfate and water is occurred. Lead sulfate is formed on plates progressively in equal quantities. Discharge process also leads to decrease in electrolyte concentration, which helps the determining the degree of discharge or controlling the state of charge of the cell.

When reverse process, charging, is occurred the high amount of lead sulfate will have been converted to lead and lead dioxide. In the case of high current of electricity flows hydrogen and oxygen gases will releases at negative and positive electrode, respectively. These gases that are in stoichiometric result in lack of water from the electrolyte (Papazov 2009)

The volume of the solid phase increases in both electrodes during discharge. When PbO_2 and Pb convert to $PbSO_4$ the volume increasing are 92% and 164%, respectively (Moseley and Rand 2004)

The battery negative electrode is one of the electrodes, which provides requirement capacity (Ah) and cold cranking ampere (CCA). It consists of negative lead grid and negative active mass that includes metallic lead and additives, such as carbon, lignosulfonate, etc.

The lead grid that is a conductor for the electricity generated in NAM supports also NAM. Corrosion is not a problem for the negative grids because it is in negative potentials throughout charge. They should have strong mechanical strength in order to

not dent during charge and discharge process. They are formed in different alloys with calcium, tin and antimony such as lead-antimony or lead-calcium-tin alloys. The common alloys are the following (Papazov 2009).

i. Pb – Sb (6.0 – 10.00%) – As (0.1 – 0.3%) – Sn (0.1 – 0.3%) – Se (0.02 – 0.03%)
ii. Pb – Sb (1.5 – 2.5%) – As (0.1 – 0.2%) – Sn (0.1 - 0.2%) – Sn (0.1 – 0.2%) – Se (0.02 – 0.03%)
iii. Pb – Sb (1.5 – 2.5%) – As (0.1- 0.2%) – Sn (0.1 – 0.2%) – Cu (0.05 – 0.06%) – S (0.005- 0.007%)
iv. Pb – Sn (0.6 – 1.2%) – Ca (0.07 – 0.09%)

2.3. Production of Negative Paste

Lead powder (leady oxide), sulfuric acid and water constitute the components of the negative paste. The paste contains 4 – 5 % sulfuric acid. The paste density is between 4.2 – 4.4 g cm^{-3} and using the density the amount of water is determined in the paste. The difference of negative and positive pastes is using additives (Papazov 2009)

Additives consist of lignosulfonate or humic acids, carbon materials (carbon black, activated carbon and graphite), barium sulfate and fiber glass. Organic compounds, lignosulfonate or humic acid, are called expander in some references while all of additives are called expander.

Negative paste is prepared in special mixers that are big and powerful. Capacity of mixers reaches up to 1000 – 1500 kg leady oxide for one paste batch. Mixers have the automatic dosage for each component and in addition to programmable control panel and cooling system. Mixing time is totally between 20 – 25 minutes.

Firstly, leady oxide and additives are added and mixed so that they mix homogenously. Secondly the water is added rapidly. If the flow rate of water is slow, the paste temperature will increase. Finally sulfuric acid is added slowly so that the temperature will not exceed the 60 ºC. When it exceed tetrabasic lead sulfate ($4PbO.PbSO_4$) will occurred, which is not in demand for negative paste.

When sulfuric acid is added to paste, an exothermic reaction commences with lead oxide (PbO) and sulfuric and result in demanded main structure:

$$4PbO + H_2SO_4 \longrightarrow 3PbO.PbSO_4.H_2O \qquad (2.4)$$

$3PbO.PbSO_4.H_2O$ (3BS) is the prismatic crystal that has a length of 1-4 μm and 0.2-0.8 μm in cross section and density of 6.5 g cm^{-3}. Solubility of this structure is very low and about 0.0262 g L^{-1}. 3BS is occurred when the sulfuric acid is added the mixer. Temperature plays an important role on kinetics of 3BS formation. When the temperature of mixing (PbO and H_2SO_4) is lower than 10 ºC, the rate of yielding 3BS is very slow (Vallat-Joliveau et al. 1995). However, between 20 and 60 ºC temperatures range 3BS occurs at high rate although paste includes small amount of unreacted PbO, which is based on the size of the PbO particles used in the beginning (Pavlov 2011e). 3BS pastes are used in negative electrode to obtain high capacity as well as longer cycle life.

$$2(3PbO.PbSO_4.H_2O) + tet - PbO + ort - PbO \longrightarrow 2(4PbO.PbSO_4) + 2\ H_2O \quad (2.5)$$

When the temperature exceeds the 70 ºC, the formation of 3BS brings to an end. After this point, $4PbO.PbSO_4$ (4BS) happens dominant phase in negative paste. It is composed of prismatic crystals that have length from 10 to 100 μm and diameter between 3 and 15 μm (Pavlov 2011b). 4BS is produced in different ways. First one is adding the H_2SO_4 solution to slurry of lead oxide and water and keeping the temperature 80 ºC throughout paste preparation (1966, Biagetti and Weeks 1970). Second one is mixing the leady oxide and H_2SO_4 solution at temperature higher than 80 ºC for at least 30 minutes (Pavlov and Papazov 1976, Iliev and Pavlov 1979). Third one is curing 3BS pastes at temperatures above 80 ºC in a purging water steam for 3 – 5 hours. By this method, the big 4BS crystals obtained but the formation is very slowly. 4BS pastes are generally used in positive electrode to get the longer cycle life. SEM images of 4BS are showed in Figure 2.2. (Pavlov 2011e).

2.4. Production and Properties of Leady Oxide

Camille Fauré, in 1881, is the first inventor to suggest and developed a process to produce leady oxide for lead-acid battery industry. The process was detailed from production of lead grid to charging of negative and positive plates. In this process, the lead oxide was produced by melting lead using a reverberatory furnace then molten lead was oxidized with a flow of air and water steam.

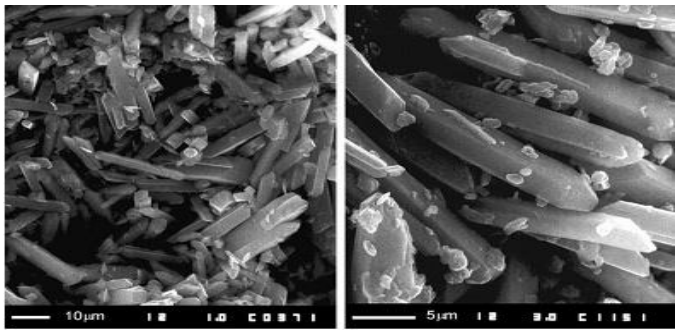

Figure 2.2. SEM pictures of 4BS crystals at different magnifications
(Source: Pavlov 2011e)

It was not suitable for production line because, the process was very slow, had taken about 30 hours, and expensive.

George Barton, in 1898, developed and patented a process. Firstly, in this new process, the melted lead was quickly stirred and formed to droplets. After that these droplets were moved and oxidized with a humidified air. Then the particles were separated according to their size, where the larger particles were sent to back reaction pot, while other smaller particles were gathered in silos. It is called Barton pot process (Figure 2.3 (b)).

G. Shimadzu, in 1926, improved a orientated ball-mill process that is used for grinding ores, pigments etc., for production of lead oxide. Firstly, the lead balls are formed. Then they are loaded and friction that would provide a significant heat to oxidize the surface of lead balls is provided by a rotational motion. After that, an certain speed of air flow and humidity is created so that it can bear away the oxide dust to silos or mill again according to their fraction of particle size (Figure 2.3(a)).

Barton pot and orientated ball-mill process are the most known and used methods. Produced lead oxide, via these methods, consists of free lead between 20% and 30%. Thus, this oxide was called ‘leady oxide’.

The leady oxide can be in two polymorphic forms, tetragonal (β – PbO), which is also dominant structure, and orthorhombic (α – PbO), which is present up to 5 - 6%. Leady oxide is the major component in lead-acid battery production when positive and negative plates are formed (Pavlov 2011a).

Table 2.1. Purity specification for lead used battery plants.
(Source: Pavlov 2011d)

Material	Flooded Battery (max wt%)
Lead	99.97 – 99.99
Trace elements	0.03 - 0.01
Bismuth	0.03
Thallium	0.01
Silver	0.005
Copper	0.0015
Antimony, arsenic, cadmium, iron, tin, zinc	0.001
Manganese, selenium	0.0005
Nickel, tellerium	0.0005[a]

[a]Quantity can be crucial in some design

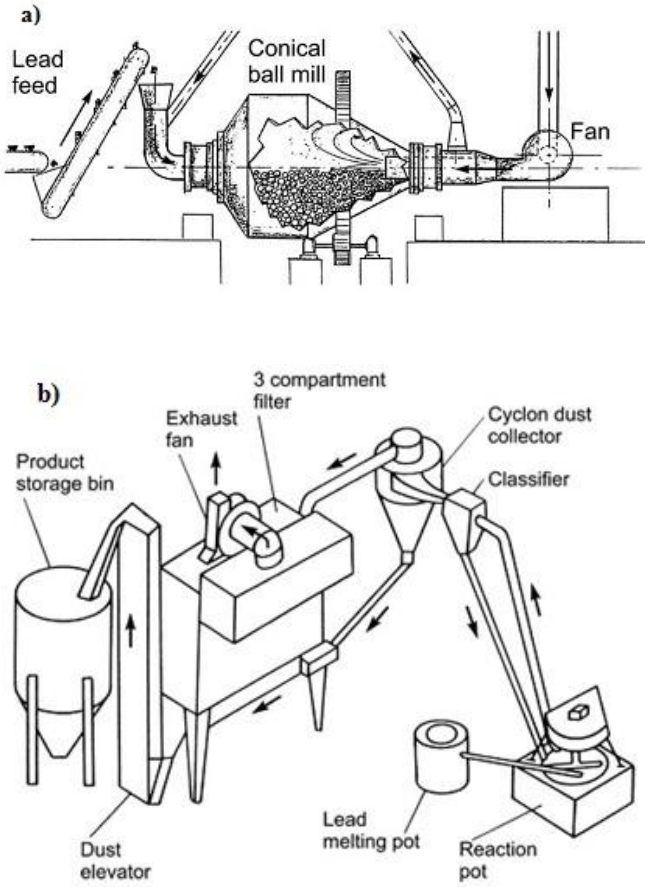

Figure 2.3. (a) Conical ball mill oxide process system (Source: Blair 1998). (b) Barton pot unit (Source: Pavlov 2011d).

2.6. Sulfuric Acid

Sulfuric acid is one of the most sold products in chemical industry. It is colorless, oily and viscous liquid with a density of 1.84 g cm^{-3}. It is soluble in water at all concentrations and this dissolution reaction is highly exothermic. Thus, the sulfuric acid is added to water, not the opposite way.

The lead-acid battery is a electrochemical system that can be easily damaged. Thus, the sulfuric acid should have a certain purity grade. Allowable amount of impurities for the sulfuric acid in lead- acid battery is summarized in Table 2.2.

The other impurities affecting the battery performance:

i. Multi-valent ions (Fe^{2+}/ Fe^{3+}, Cu^{+}/ Cu^{+2}, Cr^{+3}/ Cr^{+5}, etc.). The valency of this ions change at both electrodes thus, self-discharge rate accelerates in battery.
ii. Whole nobel metals. They decrease the over-potential of hydrogen and oxygen evolution. Hence, this reduces the effectiveness of charge and speed the battery self- discharge up.
iii. Oxidants such as ClO_3^-, ClO_4^- and $4NO_3^-$. They create soluble salts at low concentrations of sulfuric acid. These salts cause to disintegration of the PAM and NAM structures.

In addition to this, the water that is used in the electrolyte readying must be distilled and demineralized and have properties of electrical conductivity lower than 10^{-5} ohm^{-1} cm^{-1} and in the 5 – 7 pH range. Chlorine, nitrogen and sulfur compounds ought to be in quantities that are lower than detection threshold for any analytical techniques, besides metal ions precipitated with H_2S or $(NH_4)_2S$.

Dissociation of sulfuric acid occurs in two degrees. At the first degree of sulfuric acid can be shown equation (2.6)

$$H_2SO_4 \rightleftharpoons H^+ + HSO_4^- \qquad (2.6)$$

The first dissociation constant is equal to:

$$k_1 = (a_{H^+} * a_{HSO_4^-})/(a_{H_2SO_4}) \approx 10^3$$

The k_1 was determined by Young. The first dissociation of sulfuric acid is strong. Equilibrium proceeds only low amount of non-dissociated H_2SO_4.

The second degree of acid dissociation can be shown equation (2.7)

$$HSO_4^- \rightleftharpoons H^+ + SO_4^- \quad (2.7)$$

The second dissociation constant $k_2 \approx 1.02*10^{-2}$. This is signify of dissociation that is incomplete thus sulfuric acid act as weak acid.

When the first dissociation constant has high value, that is, high concentration of H^+ ions in the solution, it provides higher electrical conductivity of sulfuric acid solution in the battery. This is indispensable necessity in lead-acid battery.

Actually, the sulfuric acid does not participate in electrochemical process when electrons flow between the electrodes. It reacts with Pb^{2+} ions at two electrodes. This creates the possibility to determine quantity of electricity generated by the system indirectly. According to Faraday's law, sulfuric acid takes part during charge and discharge even though sulfuric acid takes part in chemical reaction. Sulfuric acid amount that participate in reactions at both electrode is 3.666 g when 1 Ah of electricity is delivered by the cell.

The effect of sulfuric acid concentration can be based on four basics:

i. *Open-Circuit Voltage (O.C.V).* Charge voltage of cell ought to be 40-80 mV higher than the O.C.V of a fully charged cell. In the case it is not occurred the cell will not charge fully thus, the capacity of cell will decreased and as a result of this, the cycle life reduces because of the sulfation of plates.

ii. *Electrical resistivity.* Sulfuric acid concentrations from 1.10 to 1.30 relative density, the electrical conductivity of acid is high, that is, low electrical resistivity. It provides high battery power output.

iii. *PbO_2 passivation.* When the density of sulfuric acid is higher than 1.28 g cm^{-3}, the effectiveness of PbO_2 reduces and hence, the positive plate is passivated. As a result of this, capacity and cycle life of battery will decreases.

iv. *$PbSO_4$ solubility.* When the density of sulfuric acid is higher than 1.28 g cm^{-3}, the solubility of $PbSO_4$ reduces. Hence, battery charge acceptance reduces and battery is not fully charged and as a result of this cycle life will be lower due to sulfation of plates.

Three active materials, Pb, PbO_2 and H_2SO_4, show the lead-acid battery performance with their utilization coefficients. When the sulfuric acid has the higher utilization coefficient than other compounds the battery will show the higher reversibility during cycling thus, battery will have longer cycle life. When Pb and PbO_2

have the higher utilization coefficient, the initial capacity will be high while the cycle life of battery will be lower (Pavlov 2011c).

Table 2.2. Purity requirements for battery acid
(Source: Pavlov 2011c)

Impurity	**Maximum value, (mg L^{-1})**		
	VDE 0510	**Fed.Spec. SO-801**	
Density	**1.17 to 1.30**	**1.40**	**1.28 (kg L^{-1})**
Platinum	0.05	(-)[a]	(-)
Copper (Cl)	0.5	30	50
Other metals of the H_2S group			
Singly	1	0.5	0.5
Total	2	(-)	5
Chromium, manganese, titanium	0.2	1	0.2
Singly			
Iron	30	30	120
Other metals of the ammonium sulfide group			
Singly	1	(-)	(-)
Total	2	(-)	(-)
Halogen, total	5	0.5	120
Nitrogen, as NH_3	50	5	60
Nitrogen in combined form	10	3	(-)
SO_2 or H_2S	20	(-)	(-)
Volatile organic acids:			
Acetic acid	20	(-)	(-)
Permanganate number	30	(-)	(-)
Residue on ignition at 700 to 800 °C	250	150	(-)

[a]Not specified

2.6. Negative Paste Additives

Negative paste composed of leady oxide and additives. The latter is added to improve paste physical and chemical properties of paste. They are inactive in the paste and no have solubility in other compounds. Manufacturers are interest in how additives such affect the properties of negative paste. Hence, all over the world researchers try to elucidate what the mechanism of these additives is.

2.6.1. Lignosulfonate

After the Second World War, wooden separators used in the production of lead-acid batteries were replaced by synthetic polymer materials. Because of this replacement, a drastic decrease in battery capacity and cycle life was shown at low temperatures. Researches revealed that this was due to the absence of lignosulfonate which were (previously) leached from the wooden separator into the electrolyte. After that, battery manufacturers commence to add salts of lignosulfonic acid to the negative paste.

A lot of sulfonate derivatives of lignin that have the property of surfactant properties are extensively used. Some of them are presented in Table 2.3.

Generally, these are by-products or waste products of the papermaking or wooden industries.

Lignosulfonates are strong antiflocculents. They consist of a large organic part (R^+) which is hydrophobic and a small inorganic fraction (SO_3^-) which is hydrophilic. They are soluble in water, i.e. (Boden 1998).

$$RSO_3Na = RSO_3^- + Na^+ \quad (2.8)$$

The hydrophobic part of the RSO_3^- anion will be adsorbed on the surface of the lead particles. The other part of the anion comes out to the aqueous electrolyte phase

whereby, an increasing repulsion potential is shown, which prevents the particles from coalescing or sintering (Boden 1998).

Table 2.3. Some of the products used as organic compounds of the expander (Source: Papazov 2009)

Commercial Name	Content of Material
BNF	Beta-naphthol formaldehyde condensate
DD5	Blend of Kraft lignin and condensed naphthalene sulfonate
Indulin AT	Natural wood lignin
Kraftplex	Sulfonated modified Kraft lignin
Lignotech D-1380	Partially desulfonated sodium lignosulfonate
Lomar B	Naphthalene sulfonate
Maracell XC-2	Partially desulfonated sodium lignosulfonate
N17	Sodium lignosulfonate
Vanisperse A	Partially desulfonated sodium lignosulfonate

During the years, how lignosulfonate effect on lead-acid battery negative plates have studied by lots of researchers. It was found that they adsorbed on the negative active material (spongy lead) and on the surface of lead sulfate crystals that are formed during discharge. Because of this, the crystal growth is prevented during dissolution/precipitation process. When it is not used, different centers of crystallization are created and a thick sulfate layer is formed on negative active mass. Finally, there will be no reacting lead (Aidman 1996).

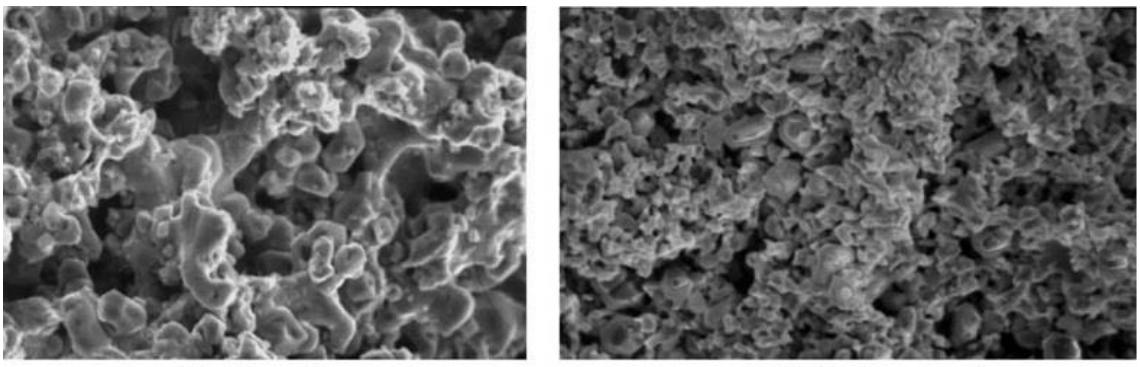

No Organic 0.5% Vanisperse A

Figure 2.4. Effect of lignosulfonate on the negative material crystal structure (Source: Boden 2004)

Moreover, preventing this growth it obtains the formation of desired structure in negative plate, tribasic lead sulfate, during curing process. This crystal structure is determinative in active mass in terms of amount of energetic and skeleton structures (Myrvold 2003).

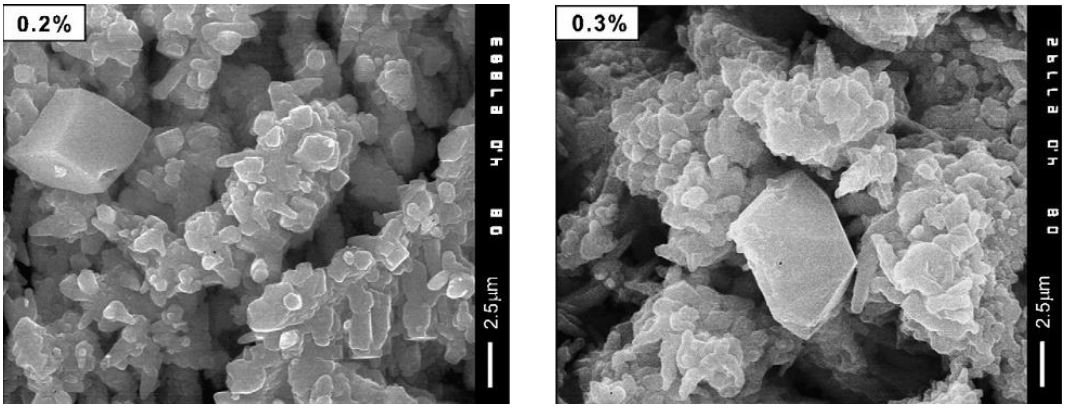

Figure 2.5. SEM micrographs of negative active masses with 0.2 % and 0.3 % of lignosulfonate (Source: Pavlov, Nikolov, and Rogachev 2010a).

However, it is claimed that lignosulfonate suppress substantially the charge process. When the spongy lead contains 0.2% lignosulfonate all of lead surface will not be covered and charge reaction proceeds easily, while in plates reaches with 0.3% lignosulfonate the surface is fully coated (Figure 2.5.). Hence, polarization of negative plate increase, then charge process is blocked, which is given rise to sulfation of the plates. Finally, the number of cycle life is decreased (Pavlov, Nikolov, and Rogachev 2010a) (Figure 2.6.).

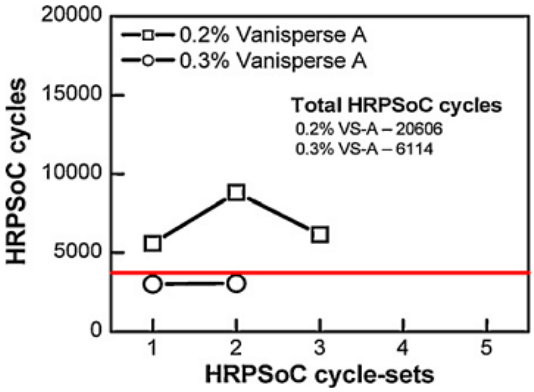

Figure 2.6. Completed HRPSoC cycles with 0.2% and 0.3% of lignosulfonate (Source: Pavlov, Nikolov, and Rogachev 2010a)

2.6.2. Carbon

Carbon materials are used as additives in lead-acid batteries lots of years. However, there is no certain information in literature how it works exactly, although many results of researches were published by investigators.

In battery industry, carbons and graphites are usually preferred as carbon materials. Carbons are carbon blacks, activated carbons and graphites, such as purified natural flake graphites, expanded graphites and synthetic spherical graphites, etc. Moreover, the carbon black is used commonly by lead-acid battery manufacturers.

Providing the strong conductivity is the most known effect of carbon materials. The surface of negative active material is covered by lead sulfate layer, carbon sustains distribution of electric current at all point of negative active material.

It has been established that using of carbon black in negative active material prevents the sulfation of negative plate. In this study, batteries had been designed for hybrid electric vehicle (HEV) applications and simulated high-rate partial-state-of-charge operations (HRPSoC) (Shiomi et al. 1997, Nakamura et al. 1996).

Specific surface area of negative active material is one of the key parameter to keep the potential of negative plates at lower than hydrogen evolution potential. However, it had been found that even if carbons that increase the surface area of negative active material they doesn't always contribute the increasing of cycle life (Pavlov, Nikolov, and Rogachev 2010b).

Researchers also try another carbon material such as activated carbon that has higher surface area while it has bigger particle size than carbon blacks. For this purpose, using activated carbon, designed a 12 V Pb – C battery to improve battery properties for

high-rate partial-state-of-charge (Xiang et al. 2013). They found that this battery had the 20% more charge acceptance than common batteries and showed more than 110,000 cycles under HRPSoC conditions. Moreover, it was established that negative plate that was formed tens-of-micron-sized carbon particles in NAM showed visibly HRPSoC cycle life than a negative plate that contains carbon or not. Furthermore, they summarize the effect of activated carbons on negative electrode:

i. Activated carbon serves as new porous-skeleton builder to increase the porosity and active surface of NAM by which assists the electrolyte diffusion from surface to inner thus, creates more sites for crystallization/dissolution of lead sulfate.
ii. Activated carbon behave like capacitive buffer to absorb excess charge current may be happen in another situation, cause to inadequate NAM conversion and hydrogen evolution.

In another study, how activated carbon affects the NAM properties, addition of carbon alters the structure of NAM. When carbon added, specific surface area of NAM increases and median pore radius decreases. If the mean pore radius is smaller than 1 μm, skeleton structure of NAM behaves like a semi-permeable membrane. Hence, this structure will suppress the access of SO_4^{2-} ions to the pores in the bulk of NAM. Because of electrochemical oxidation, Pb^{2+} ions are formed in the pores which are charged with positive charges. Providing the electro-neutrality, H^+ ions migrate from the pore solution to the bulk electrolyte and pores that are in solution gets alkalized (Pavlov and Nikolov 2013).

As for the amount of using carbon black in NAM, according the experimental results the content of all carbon material in used batteries should not exceed the 0.2-0.5 wt.% (Pavlov, Nikolov, and Rogachev 2011). They were also published that when the size of carbon particles is in nano range they are integrated into the bulk of the skeleton branches of NAM. The SEM images of the one of the carbon used are the following (Figure 2.7). As it seen that when the content of carbon is higher than 0.5 wt.%, they are incorporated into the bulk of lead. Hence, electrical parameters of NAM, such as capacity and cycle life will be damaged extensively.

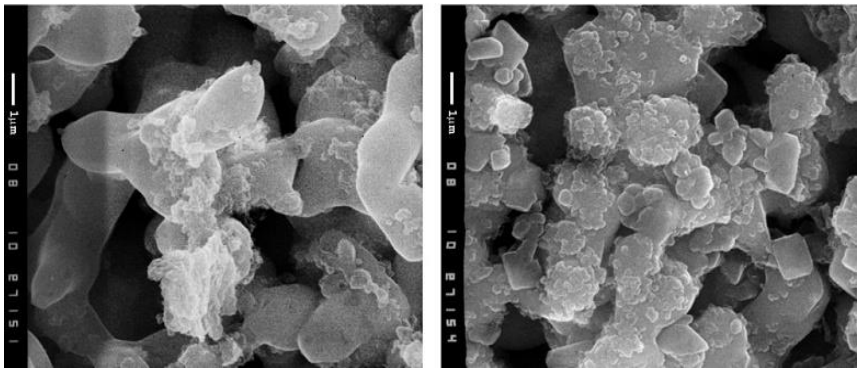

0.5% PRU + 0.8% $BaSO_4$ **1.0% PRU + 0.8% $BaSO_4$**

Figure 2.7. SEM images of NAM with 0.5 and 1.0 wt.% Printex U (PRU) carbon black (Source: Pavlov, Nikolov, and Rogachev 2011).

Although researches about carbon materials, especially about carbon black, are also in progress, new materials are investigated to replace with commercial carbon black. In situ formed carbon from sugar as additive was improved. It was reported that this new carbon form show high performance in negative electrode and avert a irreversible formation of lead sulfate on electrode surface. In addition to this, it exhibits higher charge acceptance and cycle performance than commercial carbon blacks (Saravanan, Ganesan, and Ambalavanan 2014).

Table 2.4. Commercial carbons and graphites
(Source: Pavlov 2011f)

Product	**Manufacturer**	**Type of Material**	**Bet Surface ($m^2 g^{-1}$)**	**Particle Size**
Graphites				
Formula BT 2939APH	Superior Graphite	Purified graphite	9	10 µm (d50)
Formula BT ABG1010	Superior Graphite	Expanded graphite	24	10 µm (d50)
Formula BT ABG1025	Superior Graphite	Expanded graphite	18	28 µm (d50)
Carbons				
PRINTEX XE2	Degussa	Carbon black	910	30 nm

Black Pearls 2000	Cabot Corp.	Carbon black	1475	12 nm
VULCAN XC72R	Cabot Corp.	Carbon black	257	30 nm
PUREBLACK	Columbian Chem.	Carbon black	50	42 nm
Denka black	Denki Kagaku	Carbon black	68	35 nm
Printex U	Evonik Industrie	Carbon black	100	25 nm
Printex 90	Evonik Industrie	Carbon black	300	14 nm
NORIT AZO	NORIT	Activated carbon	635	100 μm
SO-15A	TDA Research	Activated carbon	1615	< 44 μm
Purified WV-E105	Mead Westvaco	Activated carbon	2415	8.7 μm

2.6.2. Barium Sulfate

Barium sulfate is other compound used as an additive in negative active material. It is insoluble in electrolyte (sulfuric acid solutions) and inactive in water and aqueous solution. Barium sulfate does not take part in the chemical and electrochemical reactions. However, it influences performance of the electrochemical process. It serves as nuclei agent in negative active material and provides homogenous distribution of lead sulfate during discharge by the virtue of isomorphism.

Barium sulfate has the property of isomorphism with lead sulfate ($PbSO_4$) and strontium sulfate ($SrSO_4$). All of these three compounds are in orthorhombic crystal structural group. The properties of them are listed in Table 2.5.

Table 2.5. The characteristic properties of $PbSO_4$, $BaSO_4$, $SrSO_4$.
(Source: Pavlov 2011f)

	$PbSO_4$	**$BaSO_4$**	**$SrSO_4$**
Dimensions of the orthorhombic crystal lattice, A°			

A	8.45	8.85	8.36
B	5.38	5.44	5.36
C	6.93	7.13	6.84
Cation – O bond length, A°	2.87	2.95	2.83
S – O bond length, A°	1.49	1.48	1.47

These similarities between structures promote the formation of small crystal of lead sulfate in the negative active material and prevent the formation of large crystals that are difficult to recharge.

Barium sulfate decreases oversaturation of electrolyte in the pores of negative active material because barium sulfate serves as nucleation centre over growing $PbSO_4$ crystals. Nucleation overpotential does not occur because of isomorphism. Probably, $(Pb_{(1-x)}Ba_x)SO_4$ crystals are formed. Hence, $BaSO_4$ nuclei promote formation of a porous layer of small lead sulfate crystals on the surface of lead, which facilitates the crystallization process. Because of this, it impedes the accumulation of lead sulfate layer. The porous lead sulfate layer allows the transfer of Pb^{2+} ions throughout the layer.

The SEM image shows the only $BaSO_4$ particles Figure 2.8 (a) and NAM (b) which does not contain other additives except for barium sulfate. The sites where barium sulfate are adsorbed on are between Pb particles (Pavlov, Nikolov, and Rogachev 2011).

Blanck Fix and Barytes forms of barium sulfate are used when preparing the negative paste. The former is manufactured by precipitating barium sulfate from solutions of barium salts and sulfuric acid then characterized particle size that must be about 1 μm. The latter is manufactured purified natural mineral ore. Barytes particles are in the 3 – 5 μm in size range, which make it poor for negative paste (Boden 1998)

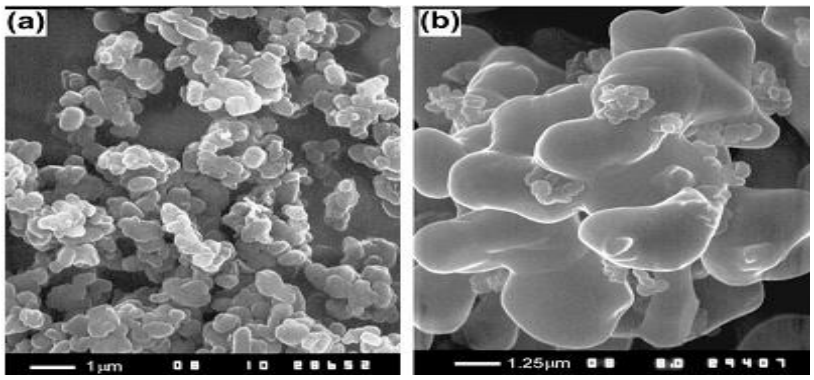

Figure 2.8. (a) SEM images of $BaSO_4$ particles (b) Adsorbed $BaSO_4$ particles on NAM surface (Source: Pavlov 2011f).

2.7. Curing of Negative Paste

Curing is the basic process in the lead-acid battery manufacturing. The goals of this process are boosting the performance properties of battery and preventing the shedding of negative active material. Throughout this process, particles are interconnected to make strong porous mass structure.

During plate curing;

i. The cured paste that has the hard porous mass is reconstructed. Small crystals transform the big ones. Water that is between particles evaporates then 3BS, 4BS and PbO particles interconnect into powerful skeleton.

ii. The remaining lead in the paste that is from leady oxide is oxidized to PbO. However, the paste contains free lead lower than 5 %.

The grid is oxidized and a corrosion layer occurs on the surface. Hence, it is provided to form strong skeleton of cured paste (Pavlov 2011g).

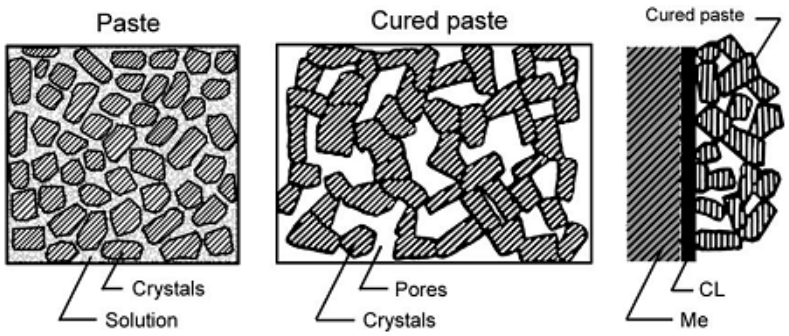

Figure 2.9. Schematic drawing of paste and cured paste
(Source: Pavlov 2011g).

This process are completed generally 40 – 50 ºC and high relative humidity (about 100%) and 18 – 20 hours. In addition to this way, there are a lot of systems used in battery technology. In these systems, temperature is high but the process time is very low, 1 – 3 hours.Final stage of curing process is drying. The aim of this step is reducing the moisture content of plate under 1%. During this step, humidity is decreased slowly and temperature is increased so that preventing formation of cracks and shedding of cured paste (Pavlov 2011g, Papazov 2009, Wagner 2009)

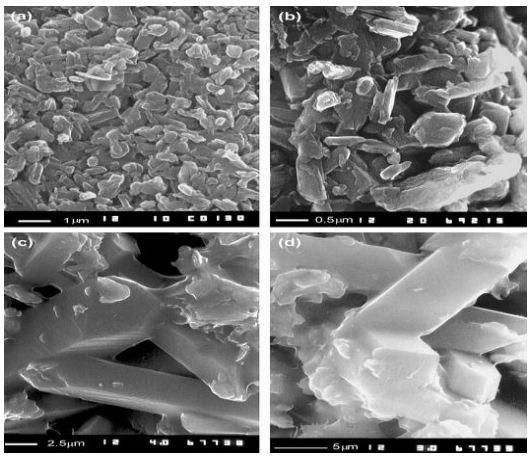

Figure 2.10. SEM pictures of cured 3BS paste (a,b) and 4BS paste (c,d)
(Source: Pavlov 2011g).

2.8. Formation Process of Plates

The cured paste consists of 3BS, PbO and very little amount of unoxidized lead and also additives such as carbon, barium sulfate, etc. This dry cured paste is an insulator and not used for current generation. Thereby, it is indispensable to convert this paste to active mass by electrochemical reactions, which is also known plate formation. Both positive and negative plates are formed in two ways. Either one is that plates are put into sulfuric acid tanks with specific gravity 1.05 – 1.15. Other one is that when battery is assembled, using higher acid concentration, with specific gravity 1.15 – 1.24, they are formed in their containers. This first step is also known soaking. Then plates are connected to electricity power source that supplies the formation currents. This value is between 0.7 – 2.5 mA cm^{-2}. This second step lasts 18 to 40 hours and

temperature should not exceed the 55 ºC. After this process, spongy lead (negative active material) on the negative electrode and lead dioxide on positive (positive active material) are formed. Formation process can be elucidated in two stages. The major components, 3BS and tetragonal PbO, are reduced to Pb and react with sulfuric acid to form $PbSO_4$ throughout first stage. These reactions participate in at low negative potential, approximately – 0.9 V, and in a reaction layer between paste and the zone of the Pb and $PbSO_4$. During second stage, 3BS and $PbSO_4$ are completely consumed and converted into spongy metallic lead (Pavlov 2011h, Papazov 2009, Wagner 2009).

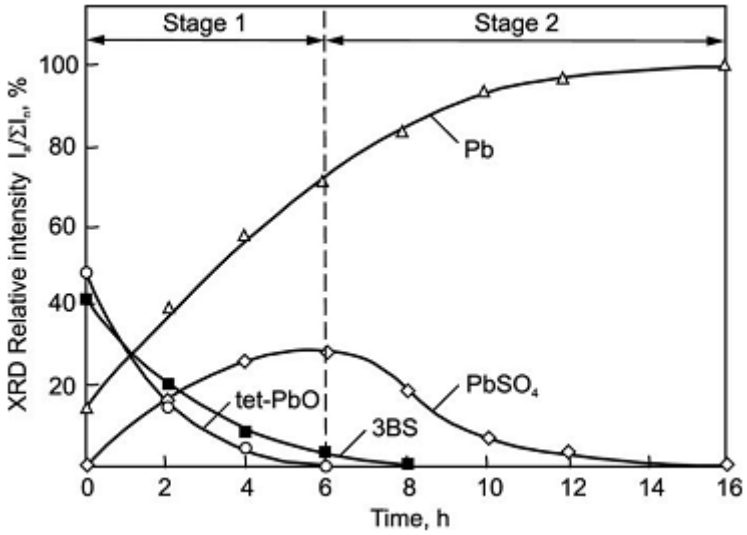

Figure 2.11. Changes on the phase composition of paste and negative plates during formation (Source: Pavlov 2011h).

2.9. A General Outlook of Electrochemical Processes

An electrochemical power source consists of two electrodes of different materials immersed in electrolyte, by which electrode systems with different potentials are formed at the two electrodes. Electrochemical reactions proceed at two interfaces which involve transfer of electrons between the electrode surface and ions from the solution. The electromotive force of the electrochemical power source is provided by differences between the potentials of electrodes. When the electrodes (anode and cathode) are connected to a conductor with a load chemical energy can be converted into an electrical one. Electric current flows thanks to transfer of valences of the materials at the two electrodes. Michael Faraday reported that, when one gram equivalent of any substance participates in an electrochemical reaction, the quantity of

electricity that flows is always equal to 96,487 coulombs (C). It is called Faraday constant and is symbolized with F.

The electric energy,Q, that is released an electrochemical reaction participate in between the electrodes is equal to:

$$Q = nF(E1 - E2) \tag{2.9}$$

where n is the number of valence of electrons that participate in electrochemical reactions, and $E1$ and $E2$ are the potential of the electrodes. The quantity of electricity is determined by F and n. Differences between the potentials of the electrodes that is made by different substances determines the electric energy. Thereby, the selection of the materials of the electrodes and electrolyte in which they are immersed is the key parameters to obtain high electric energy (Pavlov 2011b).

Gaston Planté is inventor who is combined a $Pb/PbSO_4$ with $PbO_2/PbSO_4$ electrode in sulfuric acid and achieved an electrochemical power source with high electromotive force. In 1860, it is announced by him at a meeting of French Academy of Sciences.

Some useful definitions are used battery technology the following.

Primary battery is one or group of electrolytic cells to generate electricity but no recharging.

Secondary battery is one or group of electrolytic cells to generate electricity, which has the property of recharging after fully discharged.

Anode is negative electrode of a power source, which releases electrons during discharge.

Cathode is the positive electrode of a power source, which take the electrons during discharge.

Electrolyte is a component that maintains the ionic connection between electrodes.

Separator is a polymeric material that prevents short-circuits between electrodes.

Open circuit voltage is the value of voltage between terminals of battery when there is no external current.

Closed circuit voltage is the value of voltage of the battery when battery is discharging, that is, generated current into external circuit.

Discharge is a process of the electricity generation for an external consumer.

Charge is a process of the recovery of electrodes to original form.

CHAPTER 3

MATERIALS AND METHOD

3.1. Materials

Materials, components and additives, used in experiments are detailed in the following paragraphs.

3.1.1. Leady Oxide (PbO)

The leady oxide samples used in this study (76% PbO and %24 free Pb) were obtained from a Battery Company (İnci Battery, Manisa/Turkey) using ball-milling technique to produce the oxide sample from lead whose impurities were below 0.01%.

Since the leady oxide can oxidize easily, large amount of sample, about 200 kg, was taken once and stored under argon gas in non-permeable aluminum packages that composed of two-fold polymeric material and aluminum layer.

3.1.2. Sulfuric Acid (H_2SO_4)

Sulfuric acid solutions used were purchased from Fluka, Switzerland. When the paste was prepared H_2SO_4 was added continuously for 10 minutes in winter time and for 20 minutes in summer time. The density of H_2SO_4 was diluted to 1.40 g/cm^3.

When the cured plates were charged, 600 ml H_2SO_4 was used for each cell. The density of H_2SO_4 was diluted to 1.27 g/cm^3 for formation process.

3.1.3. Lignosulfonate

Lignosulfonate with a molecular weight of 6600 g/mol used in the study was produced by Borregard Ligno Tech. and supplied by Battery Company. The impurities

and the molecular structure of lignosulfonate are given in Table 3.1 and Figure 3.1. respectively.

Table 3.1. The impurities in lignosulfonate used.

Impurities	% (max.)
Ca	0,3
Cr	0,0005
Cu	0,034
Fe	0,014
Mn	0,001
Mg	0,18
Ni	0,001

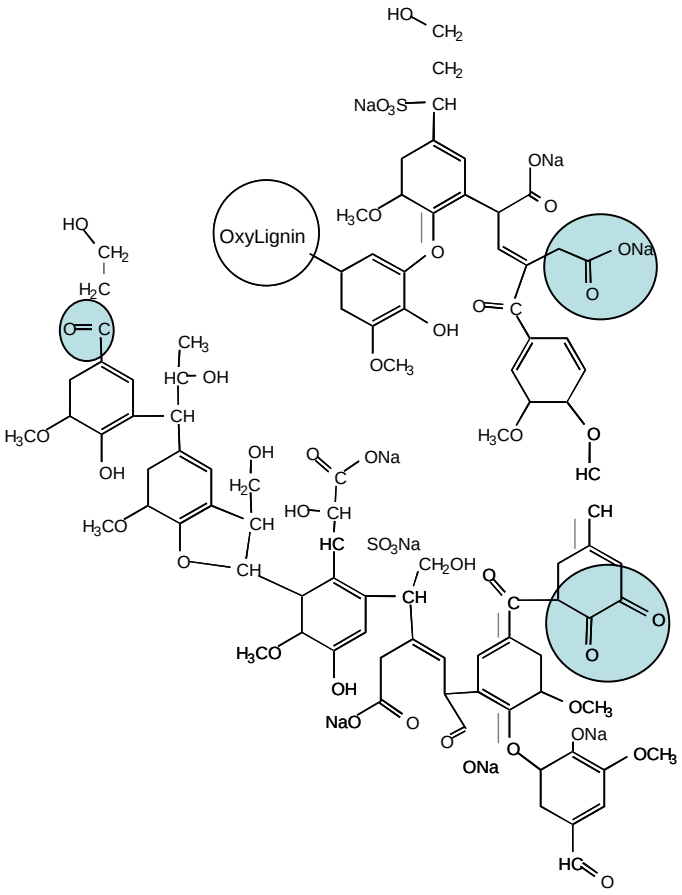

Figure 3.1. The molecular structure of lignosulfonate

3.1.4. Carbon

Several types of carbon samples that are from different producers supplied by the battery company were tested in this study. Carbon samples were also stored under argon in non-permeable aluminum packages to prevent oxidation. The suppliers and the code names (used in this study) of the carbons are listed in the Table 3.2.

Table 3.2. Definition of carbon samples used in experiments

Code	Type	Supplier
C1	Carbon Black-1	Evonik Industries, Germany
C2	Carbon Black-2	Cabot Corporation, USA
C3	Carbon Black-3	Cabot Corporation, USA
GR	Graphite	Superior Graphite, USA
AC	Activated Carbon	Cabot Corporation, USA

3.1.5. Barium Sulfate ($BaSO_4$)

Barium sulfate used in this study was a product of Solvay Chemicals from Belgium and supplied by the Battery Company. Similar to other materials, about ten kilos of $BaSO_4$ was supplied and stored under argon in a non-permeable aluminum packages to prevent oxidation. The impurities of $BaSO_4$ are given in Table 3.3.

Table 3.3. The impurities in $BaSO_4$.

Impurities	%(max.)
Ca	0,0031
Cr	0,000063
Cu	0,000046
Fe	0,00021
Mn	0,00003
Zn	0,00017

3.1.6. Fiber Glass

The fiber glass was a product of Goonvean Fibers from England and supplied by the Battery Company. The properties of fiber glass are given in the Table 3.4.

Table 3.4. The properties of fiber glass.

Raw material	Polypropilen
Length of fiber	3.0 +/- 0.6 mm
Thickness of fiber	3 Denier
Softening Point	145 +/- 5 ºC
Melting Point	165 ºC

3.2. Method

The methodology of this study is summarized in Figure 3.2. The details of the methods mentioned in this figure and the conditions applied in these methods are discussed in the following paragraphs.

3.2.1. Surface Tension Measurements

Surface tension measurements were carried out at different concentratios (10^{-2}, 10^{-3}, 10^{-4}, 10^{-5}, 10^{-6} and 10^{-7} M)of aqueous lignosulfonate solutions. For this purpose, a digital tensiometer (Krüss GmbH, K10ST) with the Du-Noüy Ring method was used. The ring is usually made up of platinum or platinum-iridium alloy of a radius (R) of 2-3 cm. The measurements were conducted at room temperature.

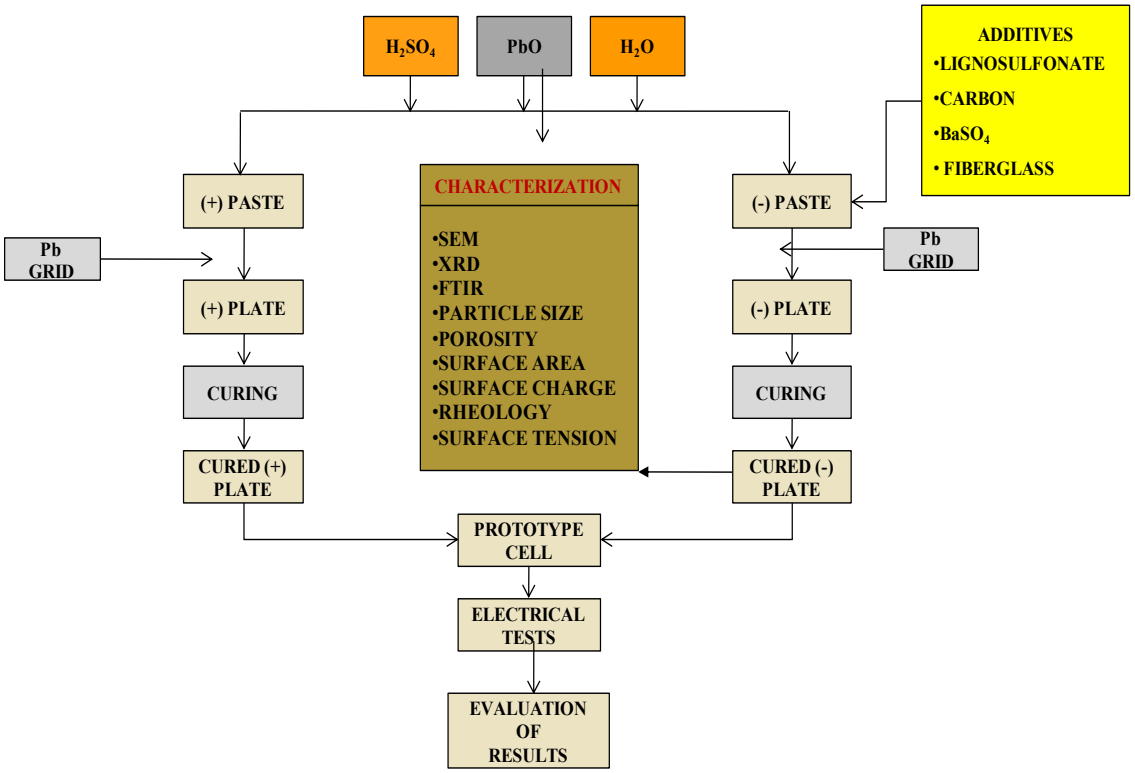

Figure 3.2. The methodology used during studies

3.2.2. Size and Charge Measurements

The particle size distributions of carbon and lead oxide particles were determined in ultrapure water and at different concentrations (10^{-2}, 10^{-3}, 10^{-4}, 10^{-5}, 10^{-6} and 10^{-7} M)of aqueous lignosulfonate solutions. For this measurements, a 0.01% carbon/lead oxide sample was dispersed using 5 mins of stirring (Carl Roth, Germnany) and then 5 mins of ultrasonic treatment (Elma, Elmasonic S 40 H, Germany) and then 5 more minutes of stirring. A light scattering device, Malvern Mastersizer 2000, was used for the size distribution measurements of well dispersed samples.

Similarly, the charge measurements of lead oxide particles were determined in ultrapure water and at different concentrations (10^{-2}, 10^{-3}, 10^{-4}, 10^{-5}, 10^{-6} and 10^{-7} M)of aqueous lignosulfonate solutions. For these measurements the same method for dispersion except calgon addition was also employed and measurements were conducted using Malvern Zetasizer Nano ZS 90.

3.2.3. Rheological Measurements

The rheological measurements were conducted using a rheometer TA Instruments AR 2000 EX. For these measurements a negative paste was prepared according to the recipe of the Battery Company explained in the following section. A 15 gram negative paste was used to conduct these measurements.

3.2.4. Paste Preparation

Two different methods were employed to prepare the pastes using the recipe of Battery Company. 1) In first method, leady oxide and the other additives were mixed as dry for 10 minutes to obtain a homogenous mixture. Then the water was added rapidly and sulfuric acid (1.40 sp. gr.) was added in 10 minutes in winter time and 20 minutes in summer time. This method was called dry mixing. 2). In second method, firstly, carbon was dispersed in lignosulfonate solution. Then, this suspension was added to the mixer fulfilling by leady oxide and barium sulfate previously. This method was called wet mixing.

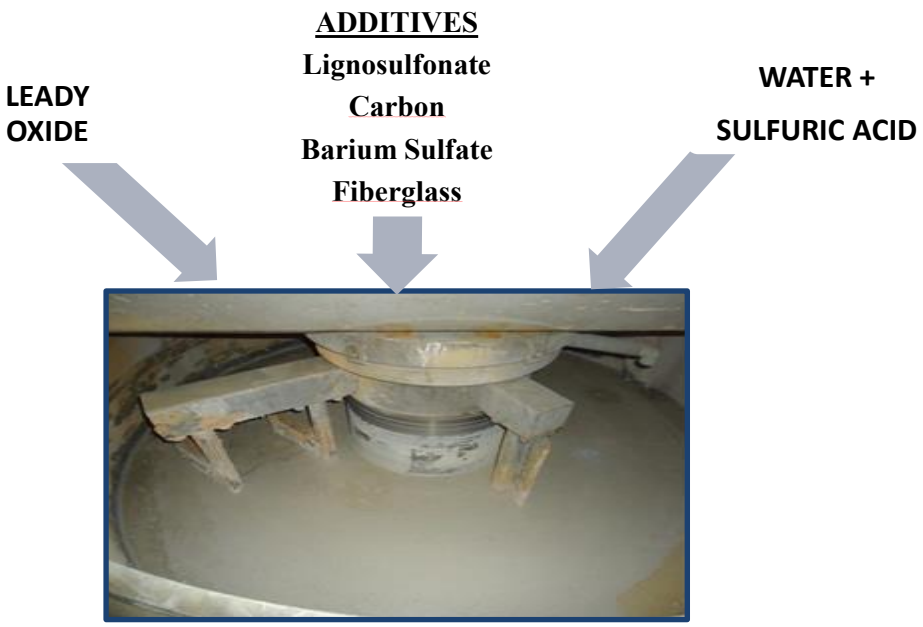

Figure 3.3. The preparation negative paste in battery plants.

3.2.5. The Preparation of Carbon Samples for SEM Analysis

The dispersed samples in pure water and in lignosulfonate solutions obtained that was explained above (in Section 3.2.2.) were used to prepare SEM samples. For this purpose a drop of dispersed suspension was placed on an aluminum sheet and freeze dried and stored in room temperature in a desiccators under vacuum.

3.2.6.Characterization Methods

Scanning Electron Microscope (Boden et al.): The SEM images of lead oxide and carbon materials, negative paste and the plates were taken to get information about the surface topography and composition. For this purpose the FEI Company-QUANTA 250FEG SEM in IZTECH Center for Materials Research and TESCAN VEGA-3SBU in battery company Center for Research and Development were both used.

X-ray diffraction: The crystal structures of negative paste and negative active material were determined by X-Ray diffraction device, Philips X'Pert Pro in IZTECH Materials Research Center. X-ray diffraction is a tool to determine the sample mineralogy and crystallography.

FTIR: Fourier Transform-Infrared Spectroscopy is a tool that is used to determine the functional groups such as alcohols, phenols, nitriles, alkynes. Shimadzu IR Prestige-21 FTIR-840 between 400 and 4000 cm^{-3} wave number range was used to determine the functional groups of the samples. The pellets were prepared 3 mg of sample and 147 mg of KBr for analysis.

Surface area analyses: Surface area analyses were achieved by Micromeritics Gemini V in IZTECH Material Research Center, which uses Brunauer, Emmet ve Teller (BET) method and nitrogen gas adsorption at 77 K.

Porosity: Porosity analyses were carried out method which is similar to liquid saturation method. Firstly cured pastes were weighed and result recorded. After that plates were waited in water bath (at 298 K), filling up the pores with water for two hours. Then, plates were weighed both in water bath and out of water bath. Difference between two cases gives the porosity value as a percent (%).

3.2.7. Paste Preparation Recipe Used in Experiments

Recipe used in experiments was taken from Battery Company, which is given in Table 3.5. Recipe is also used in company hence, the amount of components and additives was not given explicitly.

Table 3.5. Recipe used in the studies

Raw Material	**Amount**
Leady Oxide	100 kg (%70-80 PbO)
Additives	**% wt.**
Sulfuric Acid	<%10
Water	<%15
Lignosulfonate	< %0.5
Carbon Materials	< %0.1
Barium Sulfate	< %0.5
Fiberglass	< %0.5

3.2.8. Battery Performance Analysis

3.2.8.1. Reserve Capacity

Reserve capacity is the number of minutes a battery can maintain a useful voltage under a 25 ampere discharge. Reserve capacity tests were made to see the cells prepared whether they have the capacity that is expected.

Tests, which are detailed the following, were achieved according to the TS EN 50342-1.

i. Prepared cells are charged during 24 hours in 2.67 Volt. Temperatures should be between 25 °C and 35 °C.
ii. Charged cells are placed in water bath at 25 °C.
iii. Charged cells are discharged to 1.75 V with 25 A current.

iv. Discharge time (minute) represents the result, which should be higher than 90 minutes

3.2.8.2. Cold Cranking Ampere (CCA)

Cold-cranking ampere (CCA) is defined as sufficient energy to provide requirement energy to start the motor when it is cold. The amount and structure of negative active material have a huge effect on CCA.

Tests, which are detailed the following, were achieved according to the TS EN 50342-1.

i. Prepared cells are charged during 24 hours in 2.67 Volt . Temperatures should be between 25 °C and 35 °C.
ii. Charged cells are discharged to 1.00 V.
iii. Discharge time (second) represents the result, which should be higher than 90 seconds.

3.2.8.3. Cycle Life

Cycle life is a number of charge-discharge ability of battery. These tests were achieved in the company Research and Development laboratories. Firstly, prototype batteries were produced and then tests were performed. The cycle test consists of three steps as 12000, 24000 and 36000 cycles. Terminal voltage, CCA and percent of capacity were determined at the end of the each cycle number.

Figure 3.4. Prepared cells for electrical tests.

CHAPTER 4

RESULTS AND DISCUSSION

4.1. Characterization of Raw Materials Used in Paste Production

4.1.1. Surface Tension Measurements with Lignosulfonate Solutions

The forms of lignosulfonate molecules in aqueous solutions vary with their concentration. Therefore surface tension measurements were performed as a function of lignosulfonate concentration and presented Figure 4.1 (as three repeats). As seen, increasing lignosulfonate concentration reduces the surface tension up to a certain concentration. That is, surface tension reaches a constant value, Critical Micelle Concentration (CMC), which does not vary with a further increase in lignosulfonate concentration. The value obtained from these measurements is found to be around 2×10^{-3} M.

The surface tension decreased from an initial value of 72 mN/m for the no lignosulfonate case to a value of about 40 mN/m at a lignosulfonate concentration of around 10^{-3} to 10^{-2} M. Based on the results given below, the surface tension behavior for lignosulfonate could be divided into five concentration regions as Regions I, II, III, IV, V. Region I is believed to consist principally of monomers whereas Region V involves fully developed micelles. Region II, III and IV are the regions where lignosulfonate molecules are in their monomer, dimer and trimer form but the decrease in surface tension is linear. The adsorption densities in these three regions were calculated using the Gibbs surface tension equation given below.

$$\Gamma = -\left(\frac{1}{RT}\right)\left(\frac{d\gamma}{dlnC}\right) \tag{4.1}$$

where Γ and C are the surface excess and the bulk concentration of the lignosulfonate component. The area per molecule at the interface, A, can be can be calculated as:

$$A = \frac{1}{\Gamma N_{av}} \tag{4.2}$$

where Γ is the surface excess concentration at monolayer coverage and N_{av} is the Avogadro's number. The area calculated provides information on the degree of packing and the orientation of the adsorbed molecule.

From the surface tension measurements given in the above paragraphs, the adsorption density was calculated to be 1.138×10^{-6}, 1.95×10^{-6} and 5.41×10^{-6} moles/cm^2. The parking areas of single lignosulfonate molecules were calculated to be 146Å^2 between the bulk concentrations of 10^{-5} and 10^{-4} M. This means that the lignosulfonate molecules are single in solution and can be adsorbated the surface one by one. When the bulk concentration of lignosulfonate increases, the parking area decreases to 85 Å^2 and 32 Å^2 per molecule adsorbed, respectively. In these regions, the lignosulfonate molecules most probably form dimers, trimers and aggregate structures. The concentration above 2×10^{-3} M, lignosulfonate molecules reach their micelle structure and lose their ability of adsorption on paste surface. As also seen, the lignosulfonate concentration is under CMC, 1.2×10^{-5} M in the company recipe.

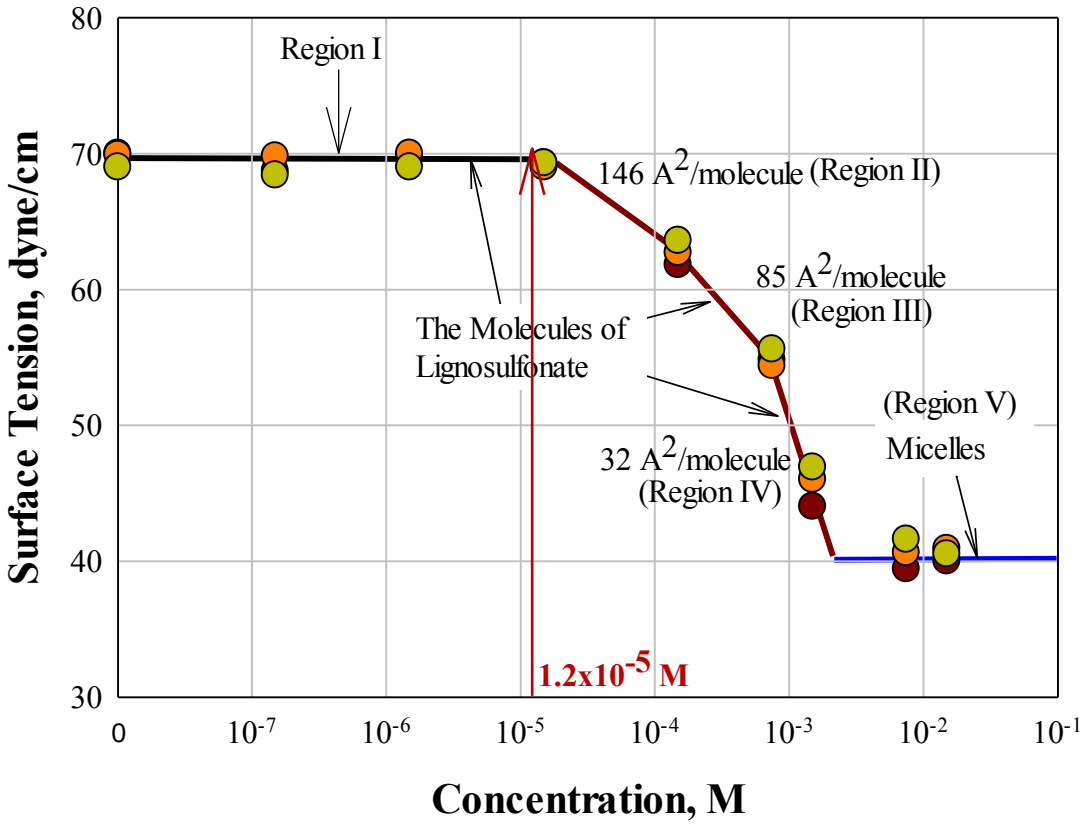

Figure 4.1. Surface tension results of lignosulfonate

4.1.2. Particle Size Distribution Measurements with Solid Materials

4.1.2.1. Leady Oxide Samples

Particle size distribution measurements of leady oxide in pure water and in different lignosulfonate concentrations, 10^{-7} M, 10^{-6} M, 10^{-5} M, 10^{-4} M, 10^{-3} M, 10^{-2} M, were performed and presented Figure 4.2. The average particles size (median average, d_{50}) of leady oxide powder was found to be about 3.5 μm in pure water. However, the size of particles further decreased only down to 3.0 μm with increasing lignosulfonate concentration up to a certain concentration, 10^{-4} M, and then started to increase again with a further increase in concentration. After CMC concentration, which is around 10^{-2} M, the particles agglomerate and become much larger (35 μm). This is most probably due to the decrease in the adsorption of lignosulfonate molecules on lead oxide surface and diminish in their dispersing agent performance after CMC. That is, they cannot perform their dispersing agent action due to lack of single lignosulfonate molecules.

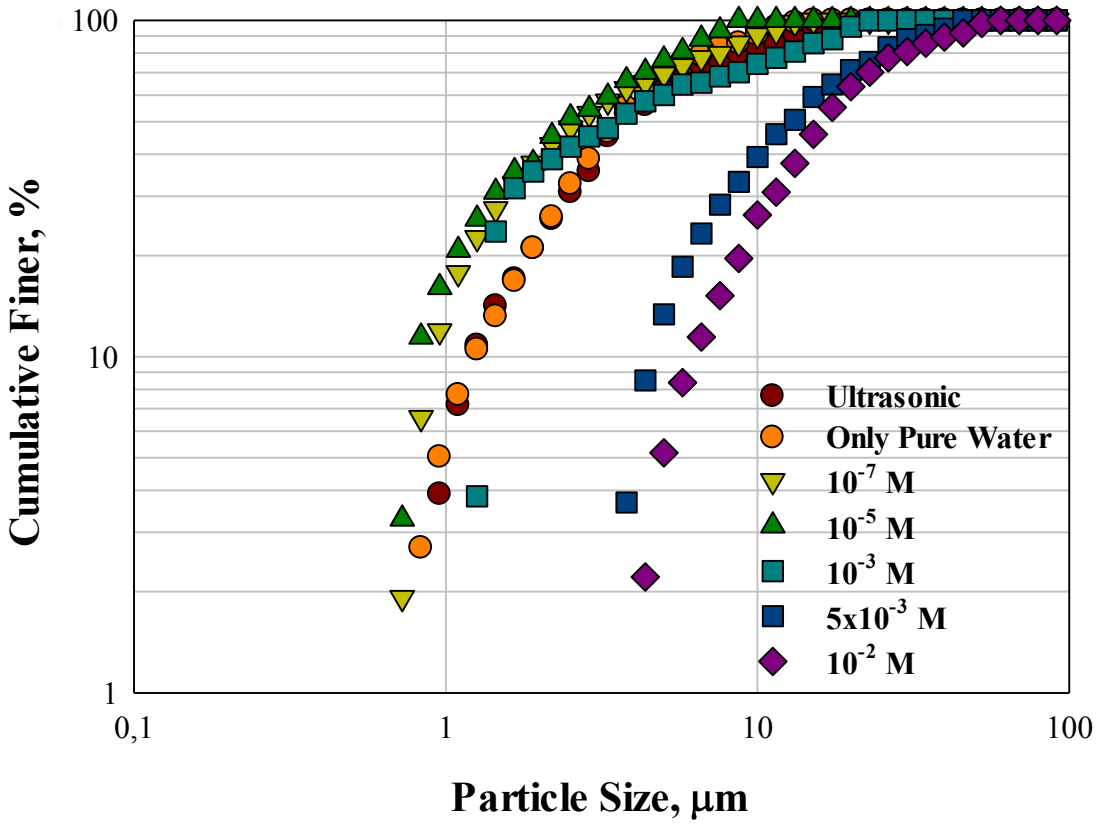

Figure 4.2. Particle size distribution of leady oxide (0.1%) in lignosulfonate solution

4.1.2.2. Carbon Samples

Particle size distribution measurements of different carbon samples that are being used as additives in paste production were performed using light scattering technique at different lignosulfonate concentrations and presented Figures 4.3- 4.8. These samples were also analyzed using SEM and these images were also presented in Figures 4.9-4.13.

As it is seen from the Figure 4.3 that the average particle size (d_{50}) of CB-1was between 1.5 and 2.0 μm and the size of 90% was around 5 μm. However the SEM images of this sample show that there is no single carbon particle and particles are strongly agglomerated. In this case, the carbon particles cannot cover the surface of negative active material (spongy lead) and show the effect expected. Moreover, this strong agglomeration can create an internal resistance in the negative active material.

In addition to the lignosulfonate, Triton X-100 (ethoxylated octyl phenol, nonionic surfactant) and L-64 (PEO/PPO/PEO Tri block co-polymer), which are known as good wetting and dispersive agents, were used to improve the dispersibility of carbon to check whether the carbon is dispersible or not. These results were also presented in Figure 4.4 together with the results of Figure 4.3 for comparison purposes.

The other carbons, CB-2, CB-3, GR, and active carbon were also presented similar results. They were agglomerated and showed no improvement or little improvement in dispersion in the presence of lignosulfonate.

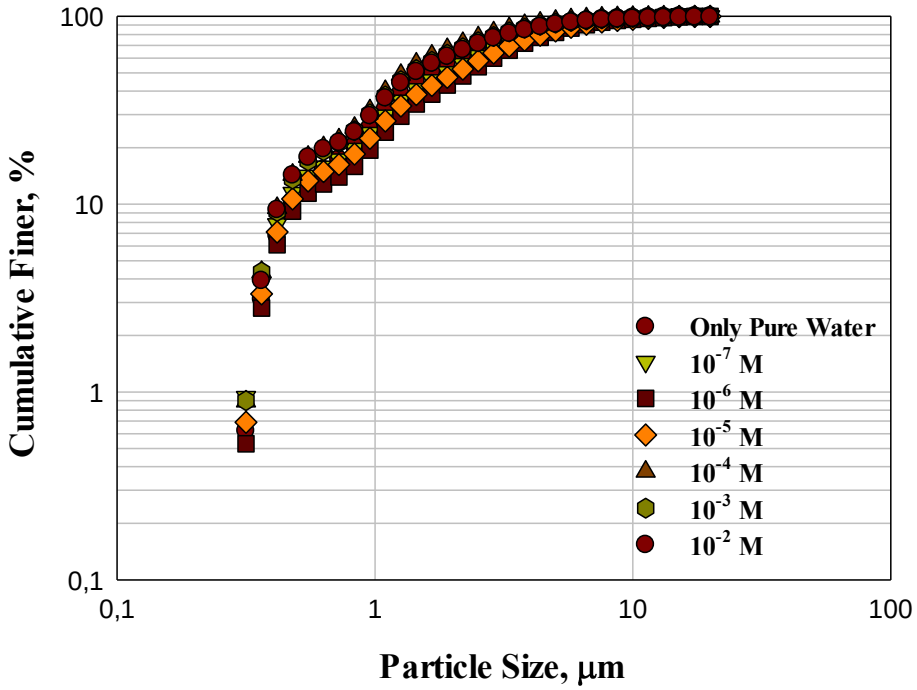

Figure 4.3. Particle size distributions of CB-1 (0.1%) in the presence of lignosulfonate solutions.

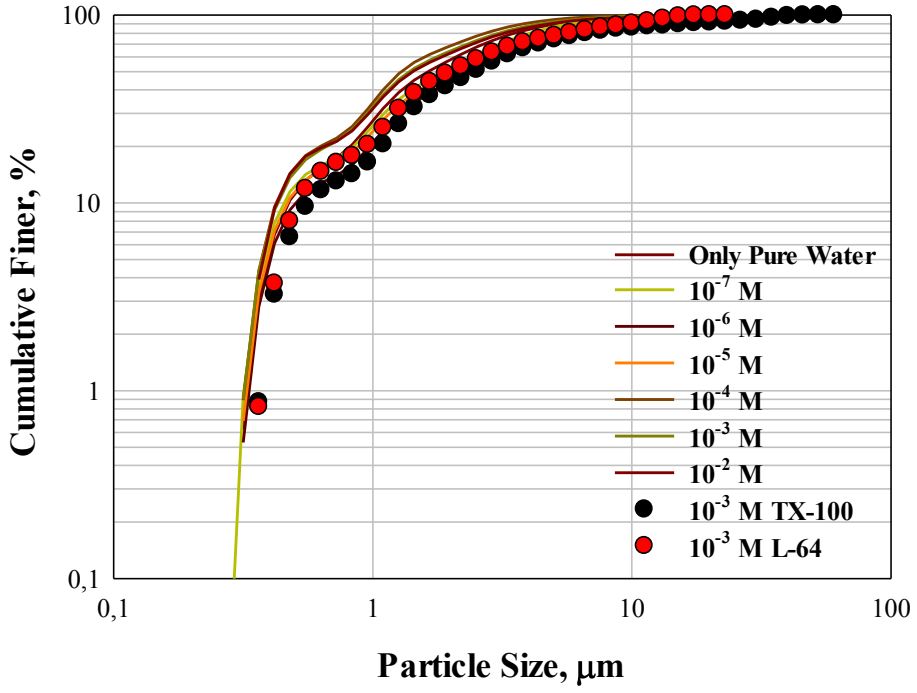

Figure 4.4. Particle size distribution of CB-1 (0.1%) in the presence of TX-100 and L-64 and comparison with lignosulfonate.

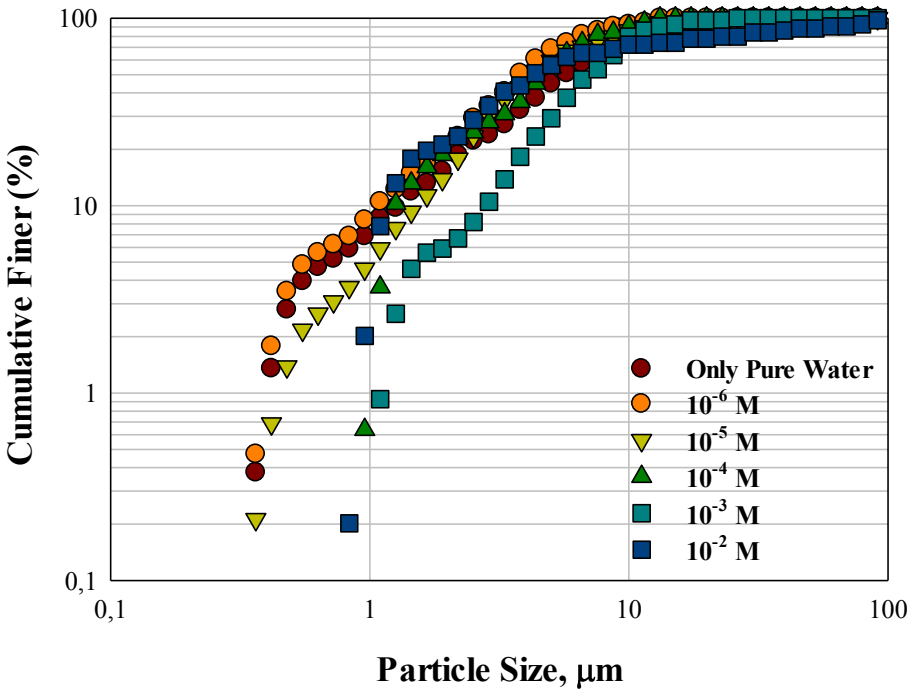

Figure 4.5. Particle size distributions of CB-2 (0.1%) in the presence of lignosulfonate solutions.

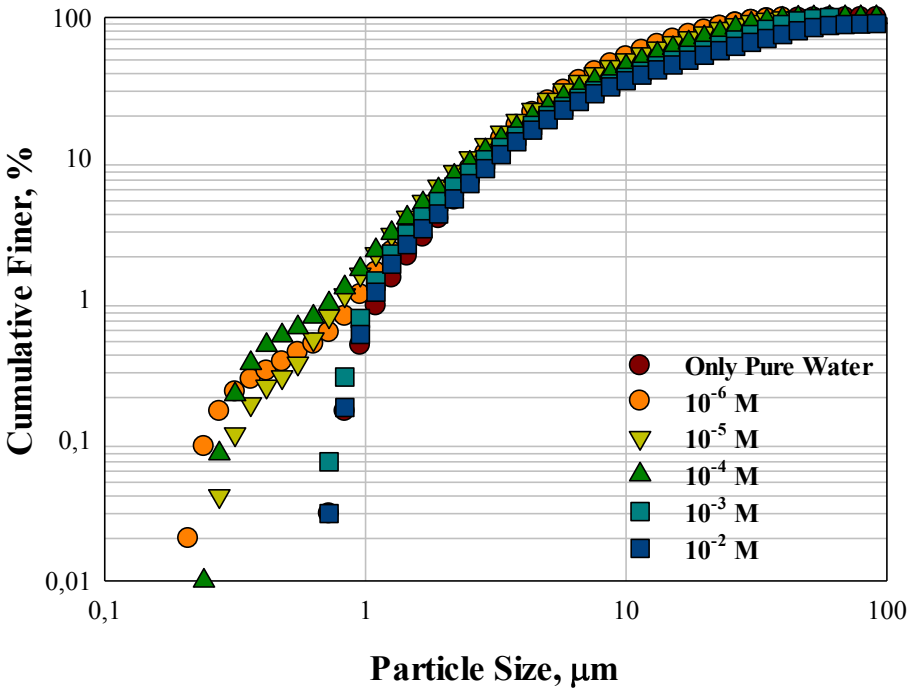

Figure 4.6. Particle size distributions of CB-3 (0.1%) in the presence of lignosulfonate solutions.

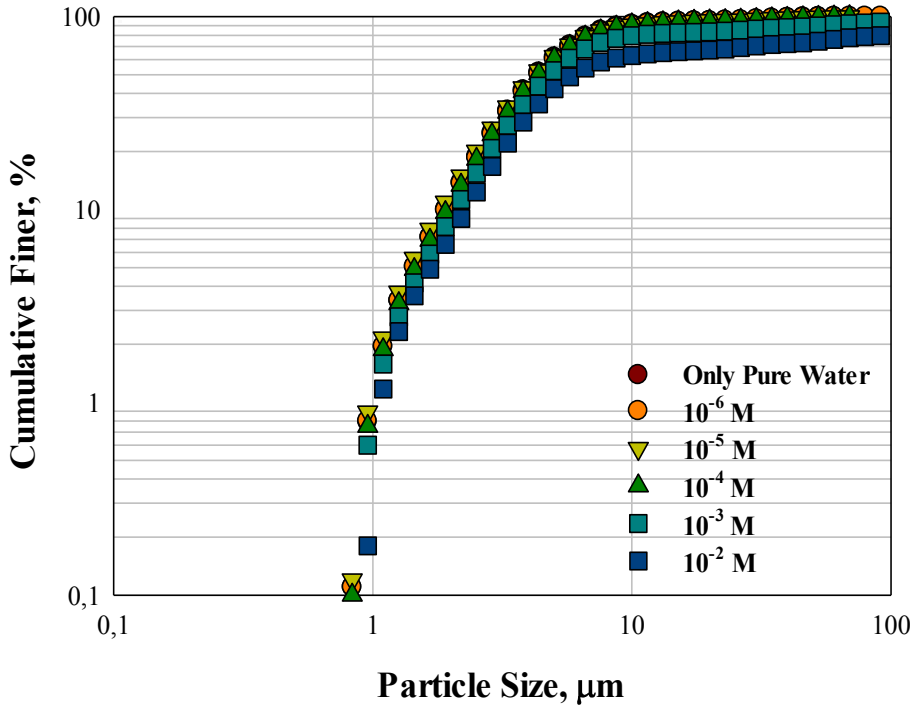

Figure 4.7. Particle size distributions of GR (0.1%) in the presence of lignosulfonate solutions.

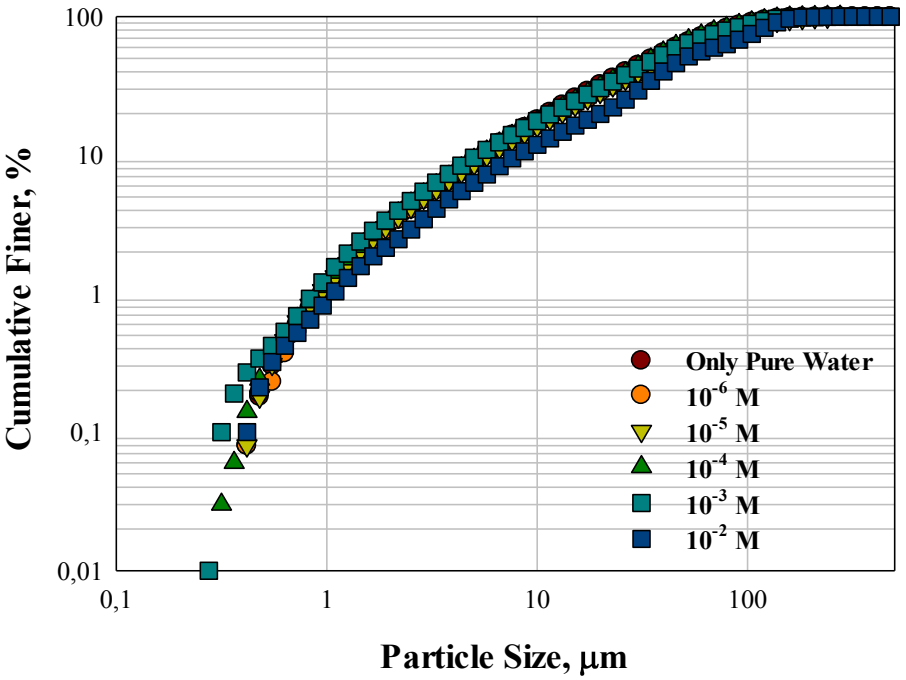

Figure 4.8. Particle size distributions of AC (0.1%) in the presence of lignosulfonate solutions.

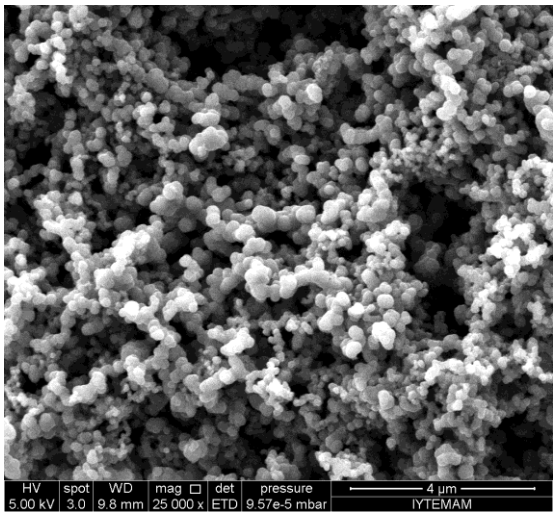

No Lignosulfonate

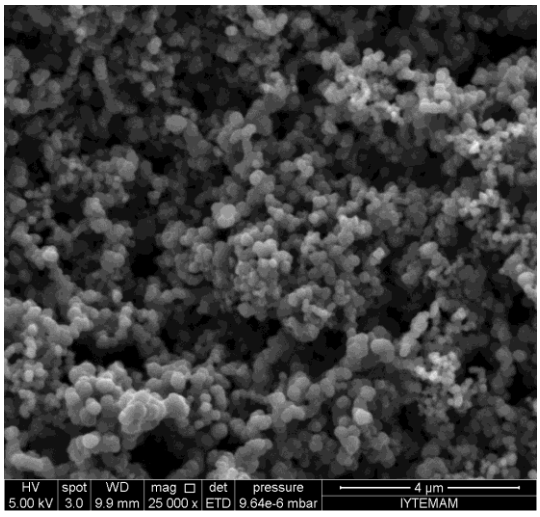

10^{-7} M Lignosulfonate

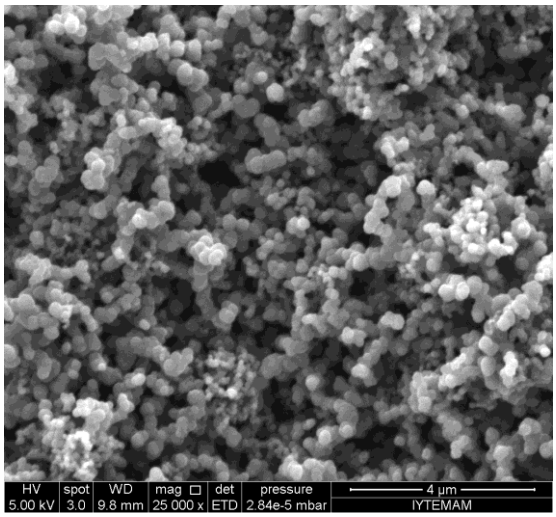

10^{-5} M Lignosulfonate

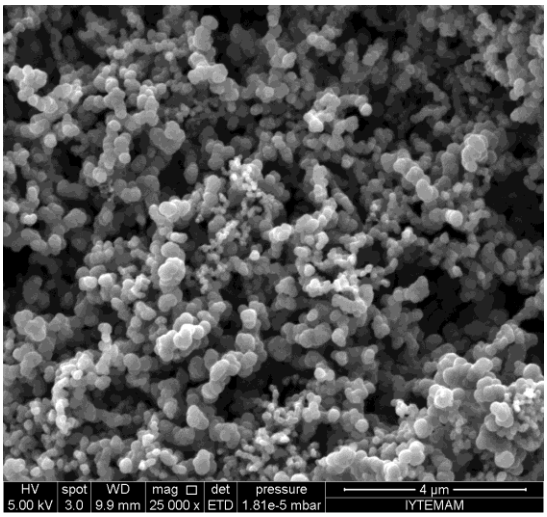

10^{-4} M Lignosulfonate

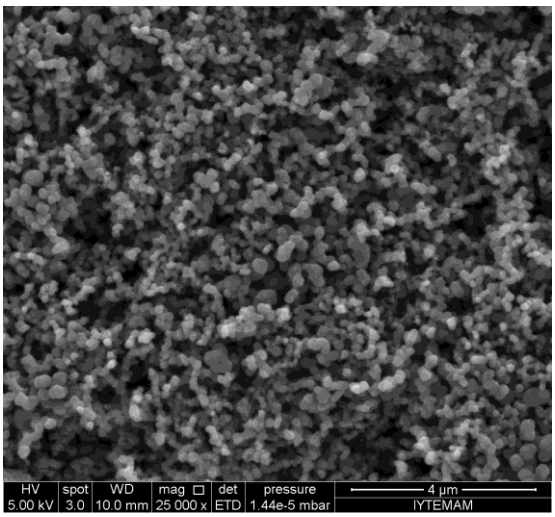

10^{-3} M Lignosulfonate

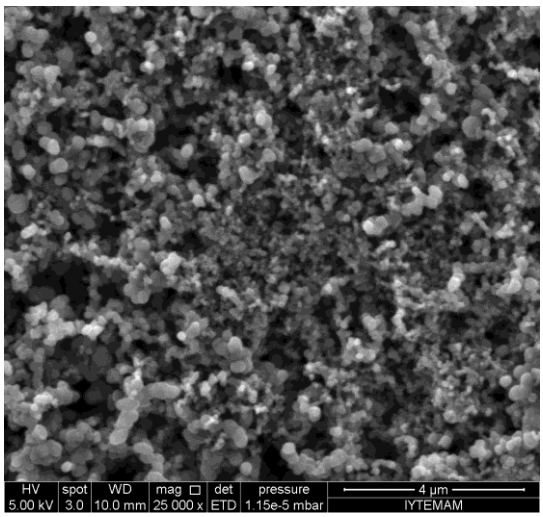

10^{-2} M Lignosulfonate

Figure 4.9. Change in SEM images of CB-1 with lignosulfonate

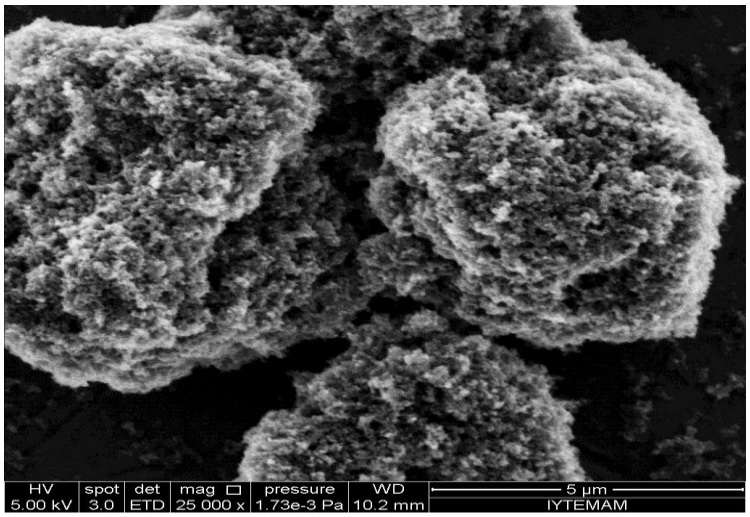

10^{-3} M Lignosulfonate

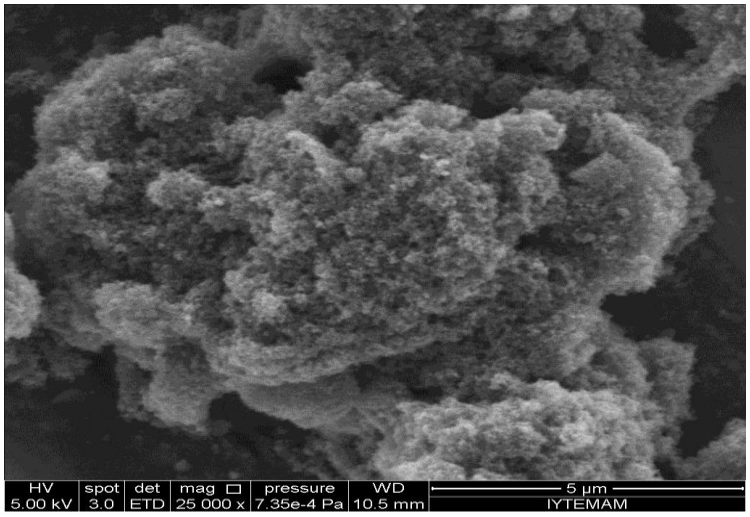

10^{-5} M Lignosulfonate

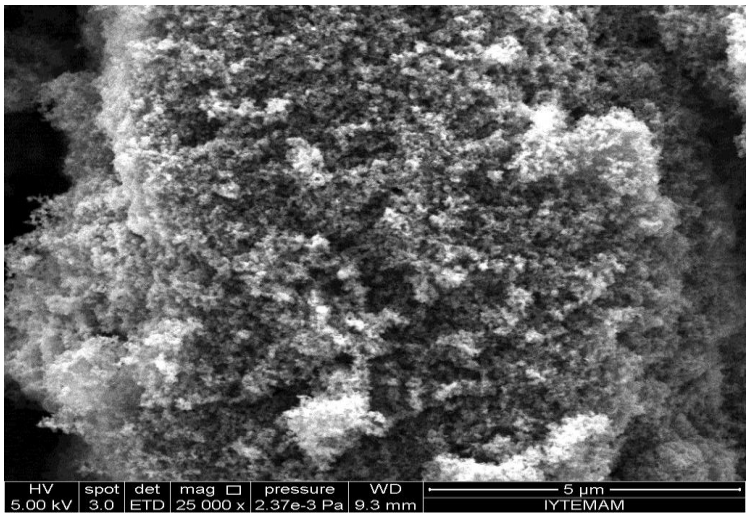

Only Pure Water

Figure 4.10. Change in SEM images of CB-2 with lignosulfonate

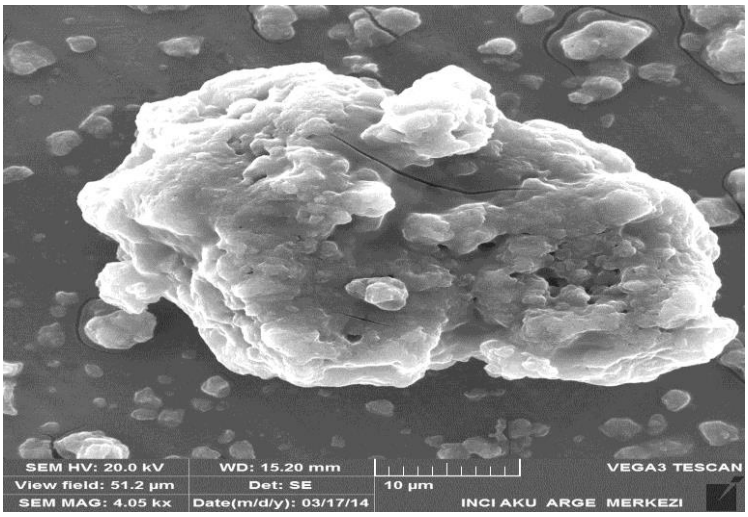

10^{-3} M Lignosulfonate

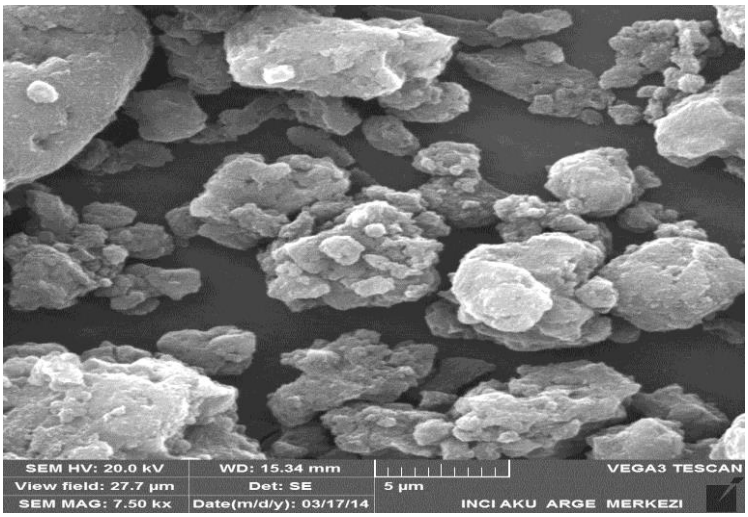

10^{-5} M Lignosulfonate

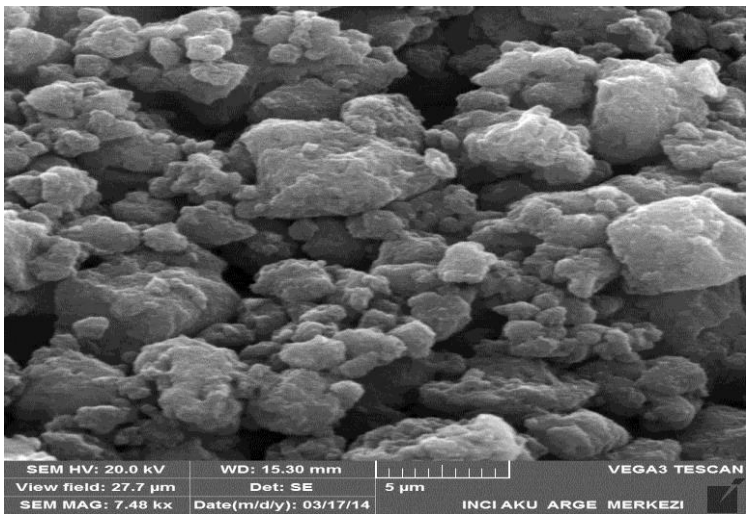

Only Pure Water

Figure 4.11. Change in SEM images of CB-3 with lignosulfonate

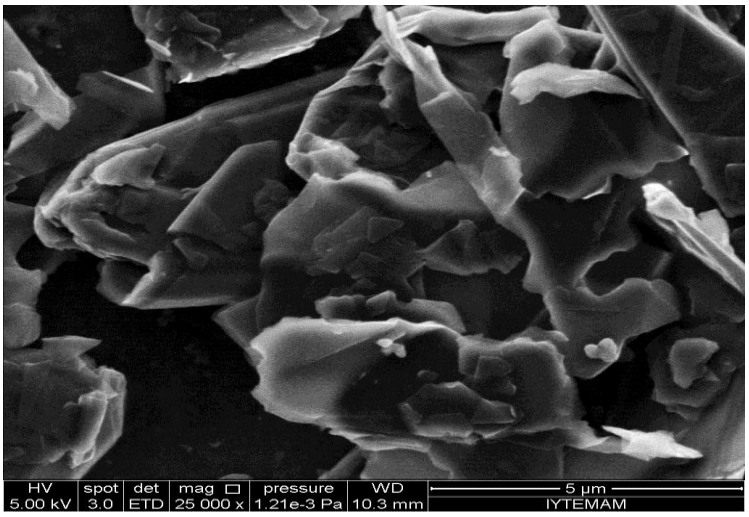

10^{-3} M Lignosulfonate

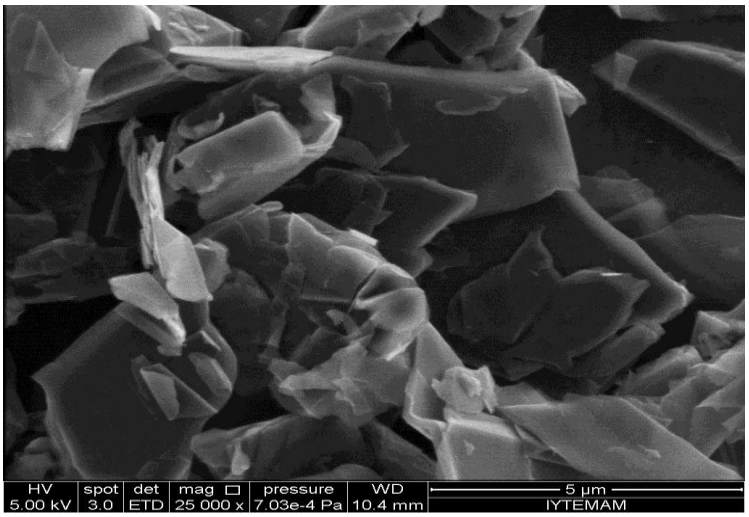

10^{-5} M Lignosulfonate

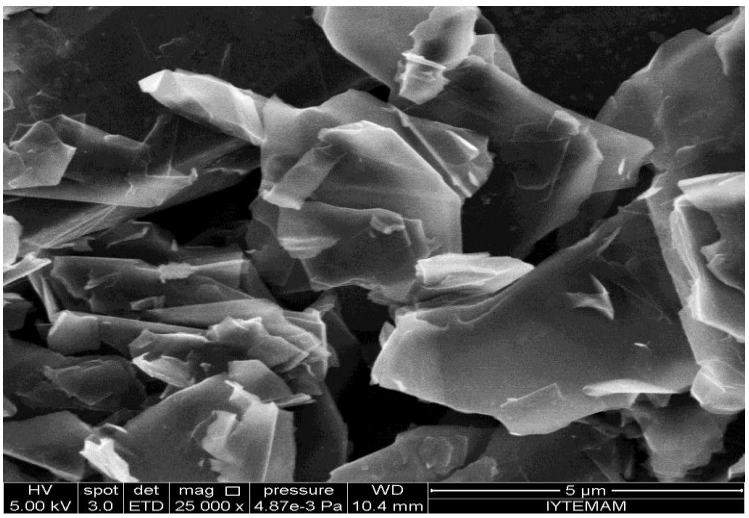

Only Pure Water

Figure 4.12. Change in SEM images of GR with lignosulfonate

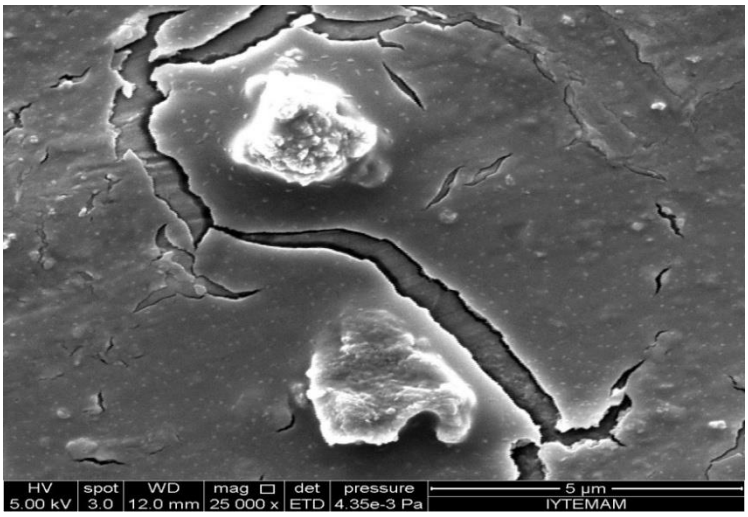

10^{-3} M Lignosulfonate

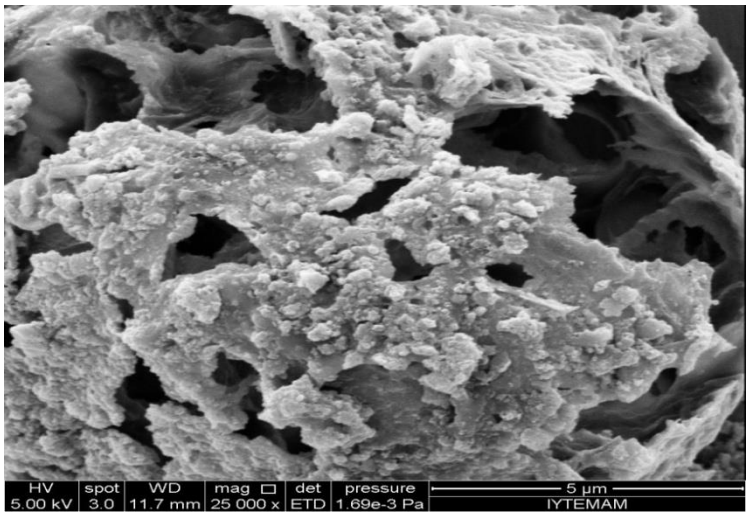

10^{-5} M Lignosulfonate

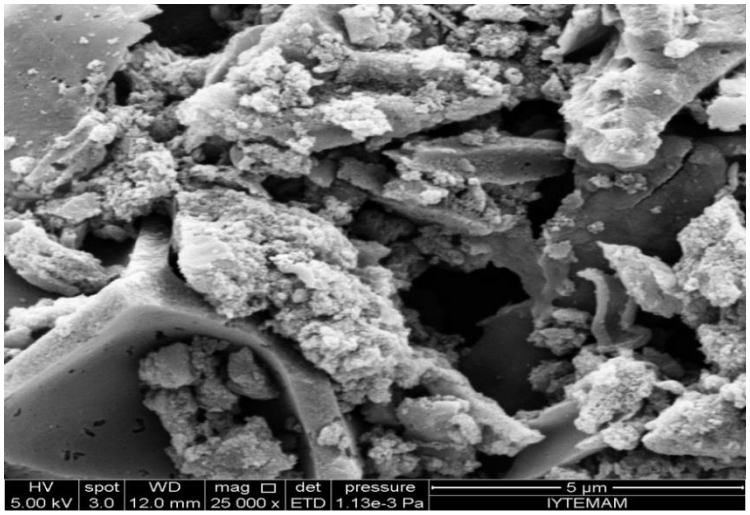

Only Pure Water

Figure 4.13. Change in SEM images of AC with lignosulfonate

4.1.2.3. Barium Sulfate

Particle size distribution of barium sulfate was performed with using pure water and result is presented in Figure 4.14. The average particle size (d_{50}) was found to be 2.2 μm.

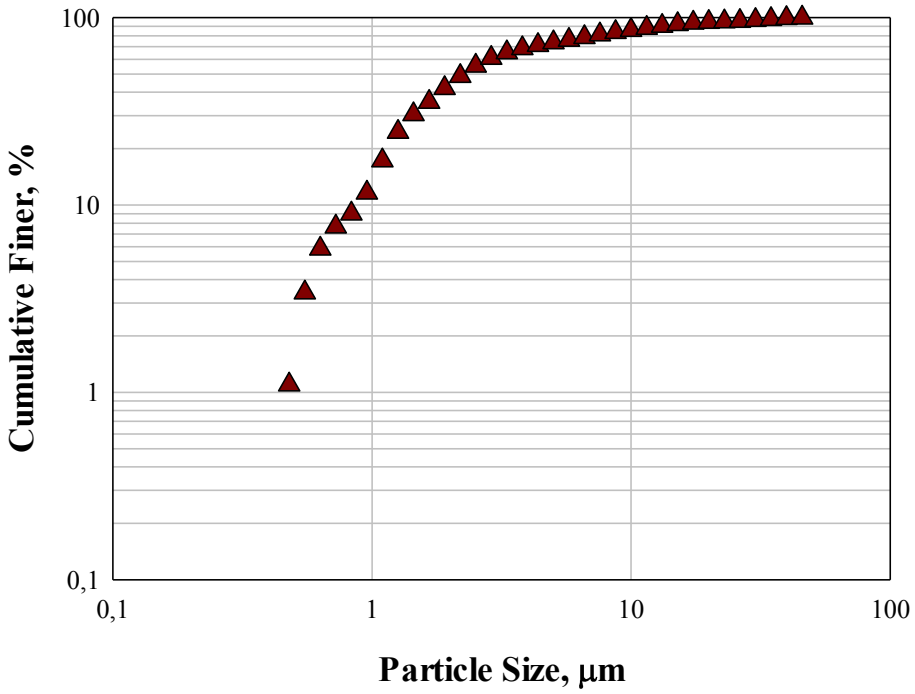

Figure 4.14. Particle size distribution of barium sulfate

4.1.3. Charge Measurements

This part of the study was design to determine the charge of lead oxide particles as a function of lignosulfonate concentration at a fixed pH value. The results are presented in Figures 4.15. However, the presence of lignosulfonate decreases positive charge down to zero with increasing concentration (up to 10^{-5} M) then becomes negative at 10^{-4} M. However, this negative charge becomes zero again at higher concentrations of lignosulfonate. This indicates the adsorption of lignosulfonate molecules on lead oxide surface and expected to affect the agglomeration behavior of lead oxide particles. The pH of leady oxide in pure water was 8 (0.1% PbO).

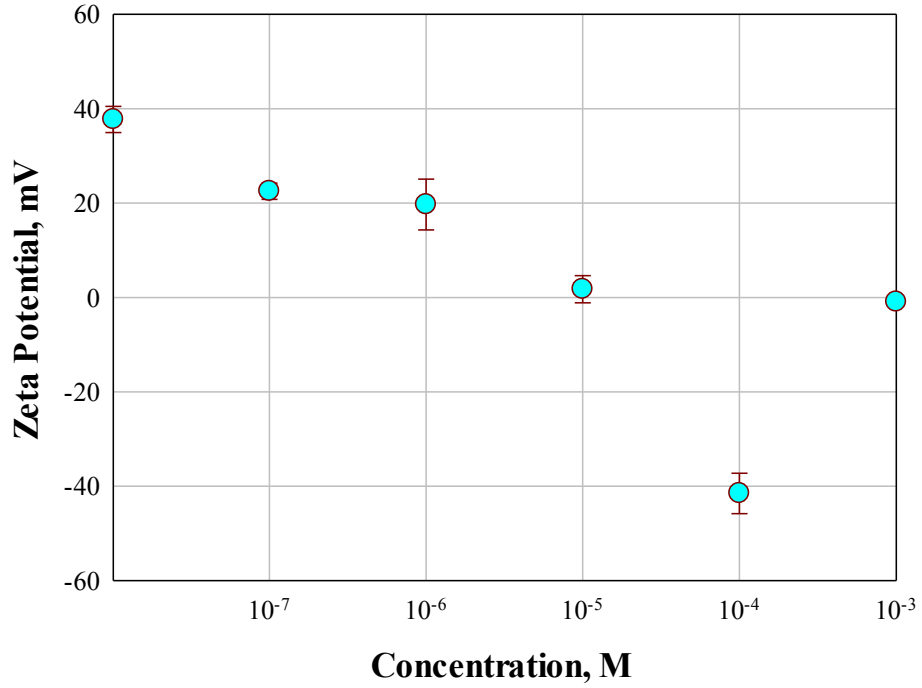

Figure 4.15. Change in zeta potential of leady oxide in lignosulfonate solution.

4.2. Characterization of Negative Paste: Rheological Measurements

The characterization of negative paste was performed to understand the effect of additives such as carbon and lignosulfonate on the homogenous structure of paste. For this purpose, rheological measurements were conducted under different conditions of additives used. Especially the way of their addition (dry or wet mixing) was important since the amounts of these additives were already studied in detail in the past and the recipes were developed. Therefore some rheological studies were conducted and discussed in the following paragraphs.

4.2.1. The Rheological Behavior of Leady Oxide Alone

First of all, the rheological behavior of leady oxide in pure water was studied using different percentages of 20%, 40%, 60% and 80%. The results are presented in Figure 4.16 as shear stress versus shear rate curves, in Figure 4.17 as viscosity versus shear rate curve and 4.18 as Viscosity versus leady oxide ratio (%).

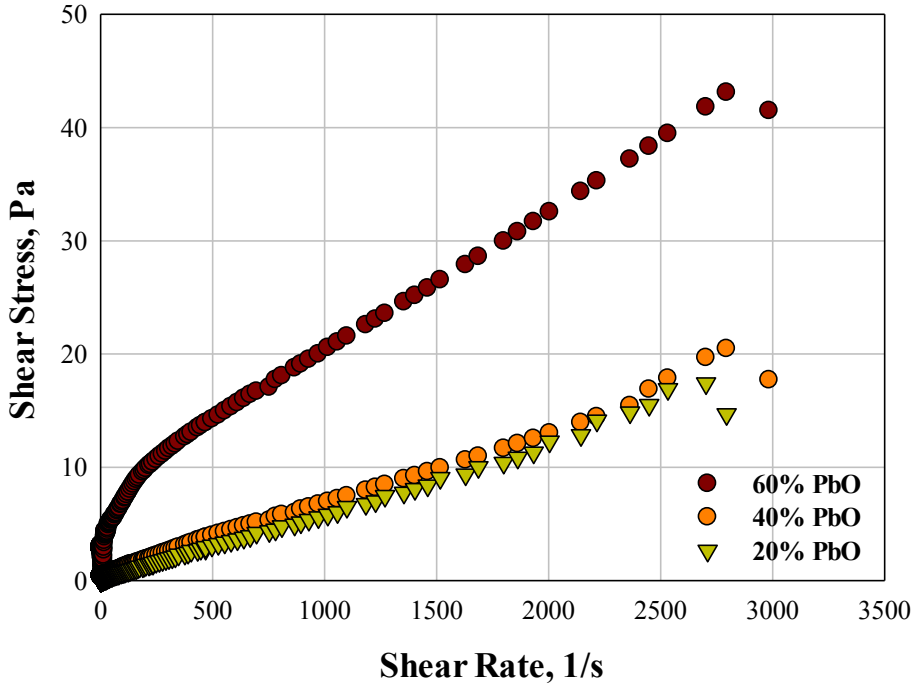

Figure 4.16. The rheological behavior of leady oxide

As seen from the Figure 4.16 that leady oxide suspensions behave a newtonian fluid for suspensions of 20% and 40% and non-newtonian over 50%.

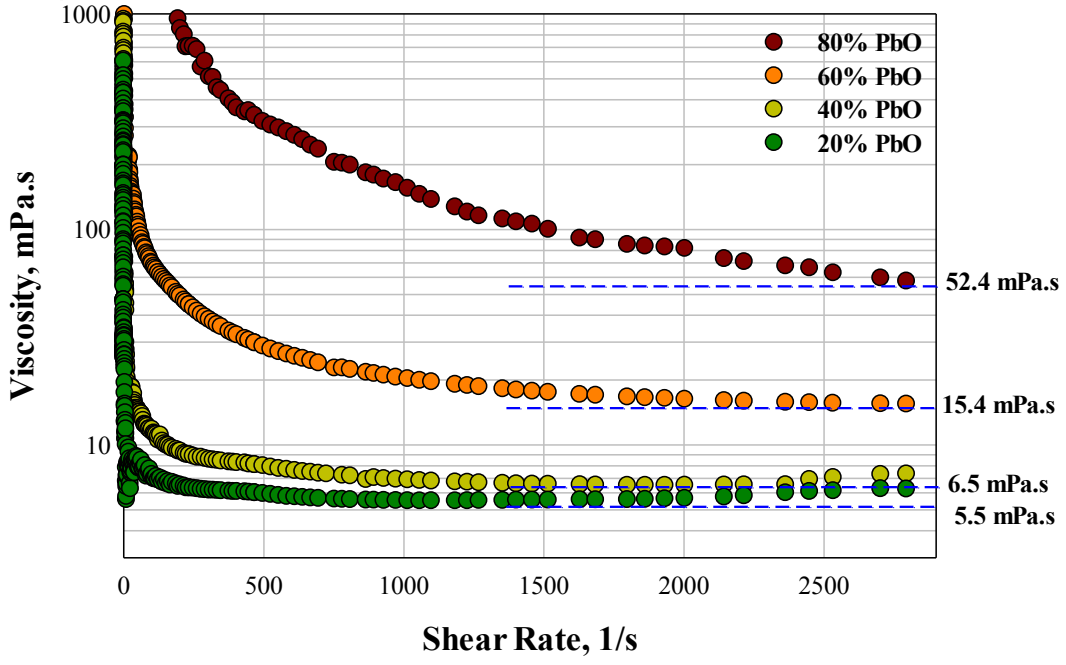

Figure 4.17. Viscosity of leady oxide in different ratio of leady oxide-water suspensions

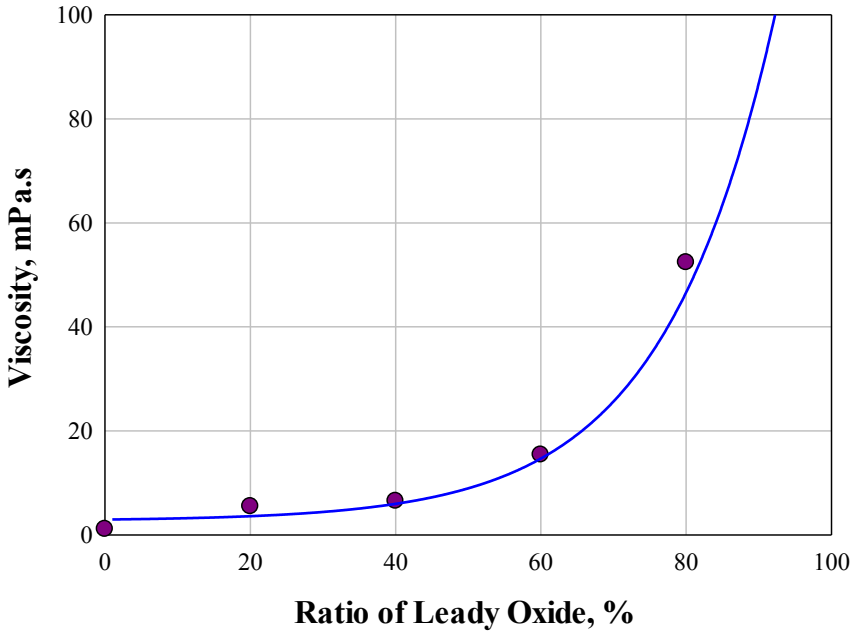

Figure 4.18. Viscosity of leady oxide in different ratio of leady oxide-water suspensions

Using the Figures 4.17 and 4.18, the viscosities of suspensions were found as 5.5, 6.5, 15.4 and 52.4 mPa.s from lowest rate suspension to highest one, respectively. These results also show a mixing time that is necessary for reaching the equilibrium which is expected to affect the quality of negative paste.

4.2.2. Effect of Dry and Mix Method

Rheological measurements of dry and wet mix method was completed and given in Figure 4.19. The viscosities of dry and wet mix were measured as 25.2 and 20.6 mPa.s respectively. As seen, the paste prepared with wet mix method has the slightly better fluidity than dry mix method. Here, the amount of whole component and additives were same with company recipe.

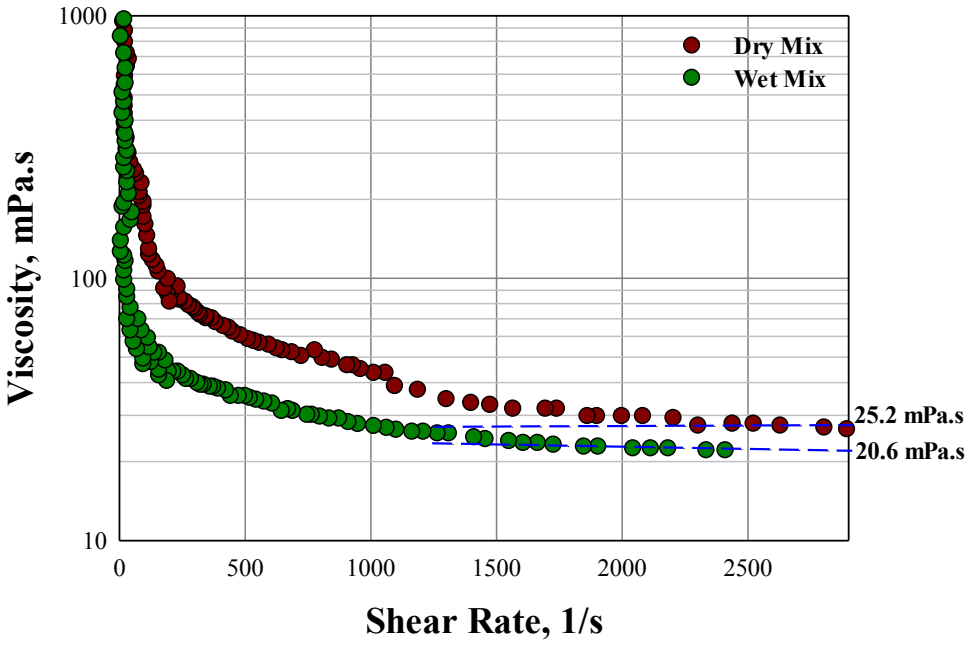

Figure 4.19. Effect of dry and wet mix method

4.2.3. Effect of Amount of Carbon and Lignosulfonate

In this part of the study, rheological measurements were conducted by changing the amount of carbon and lignosulfonate (important additives) in the mixtures. In these mixtures, carbon was dispersed in lignosulfonate solution first and then leady oxide was added and called Wet Mix (Factory), Wet Mix-1 and Wet Mix-2. These conditions were summarized in the following list and the results were discussed in the following paragraphs.

i. Carbon was dispersed in lignosulfonate solution where the amount of both carbon and lignosulfonate is the same with company, then addition of leady oxide (Wet Mix (Factory)).

ii. Carbon was dispersed in lignosulfonate concentration where the amount of lignosulfonate is 10-fold higher than company recipe but carbon same, then addition of leady oxide (Wet Mix-1).

iii. Carbon was dispersed in lignosulfonate concentration where the amount of carbon is 10-fold higher than company recipe, then addition of leady oxide (Wet Mix-2)

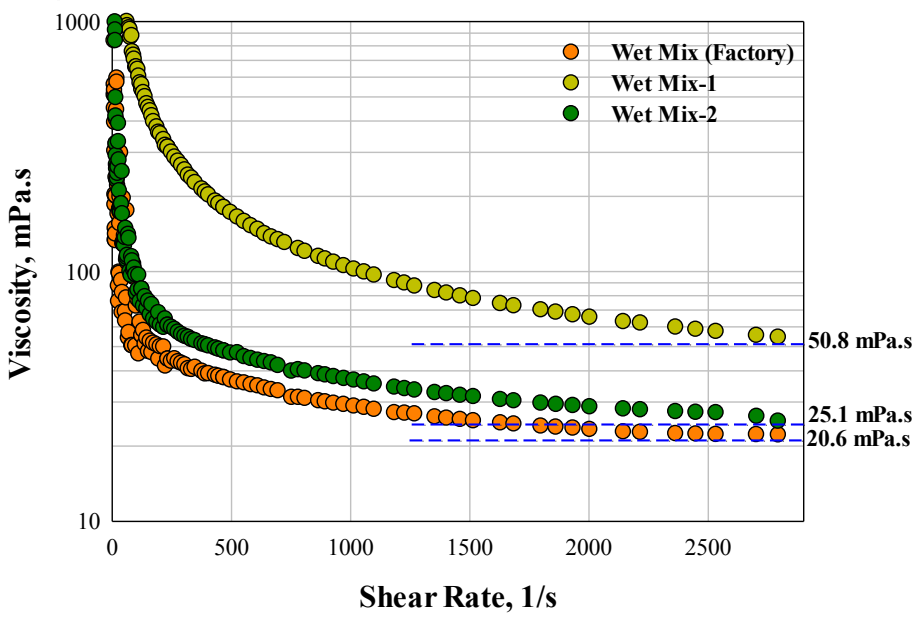

Figure 4.20. The effect of carbon and mixing type to the viscosity

As it is seen from the figure 4.20 that there are differences between the viscosities of mixture types where the amounts of carbon are different in Wet Mix (Factory) and Wet Mix-2. As given above the lignosulfonate concentration is different in Wet Mix-1, which has highest value. The viscosities of Wet Mix (Factory), Wet Mix-1 and Wet Mix-2 were measured to be 20.6 mPa.s, 50.8 mPa.s and 25.1 mPa.s respectively. It seems that there is an optimum amount of carbon to have low viscosity for the mixture.

4.2.4. Effect of Preparation Method

In this part of the study, rheological measurements were conducted to study the effect of negative paste preparation method. Therefore all the ingredients were mixed in two ways, wet or dry. The results are presented in Figure 4.21 as viscosity versus shear rate curve. These conditions of this part of the study were summarized in the following list and discussed in the following paragraphs.

i. Lignosulfonate, carbon black, barium sulfate and fiber glass was mixed and then sulfuric acid and water were added (Mix-1).

ii. Firstly, carbon was dispersed in lignosulfonate concentration then it was added to mixture which was prepared mixing of leady oxide, barium sulfate and fiber glass and finally sulfuric acid was added (Mix-2).

iii. Firstly, leady oxide was dispersed in lignosulfonate solution then it was added to mixture which was prepared mixing of carbon, barium sulfate and fiber glass and finally sulfuric acid was added (Mix-3).

As it is seen from Figure 4.21 that the viscosity of mix-2 was lower (as 20 mPa.s) than mix-1 and 3 (as 25 mPa.s). In addition to this, the mix-2 paste has the ability to reach a better fluidity in a short time. Mix-2 is wet mixture where carbon is dispersed in lignosulfonate solution first and then added to the other ingredients. Mix-1, where all the ingredients were mixed dry, and Mix-3, where lead oxide was dispersed in lignosulfonate and then added to the other ingredients, were behaved similar. That is, the preparation of a homogenous mixture that affects the viscosity, seem to depend on how to add and mix the ingredients.

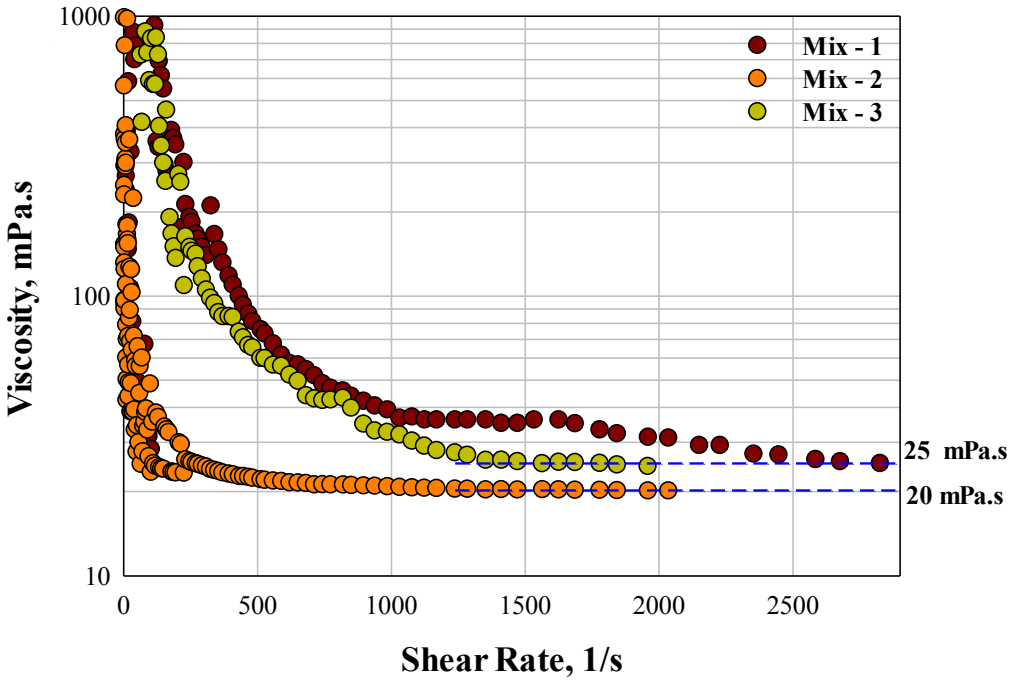

Figure 4.21. The viscosity values of prepared negative paste

4.3. Characterization of Negative Plates

Negative pastes prepared for all the conditions were spread out on grids called plates. Then all plates were cured, at 55 ºC with 100% relative humidity during 24 hours, and dried in the same conditions. The cured plates were characterized using some techniques as SEM, XRD, BET surface area, FT-IR and discussed in the following paragraphs.

4.3.1. SEM Analyses

The SEM analyses of the plates were performed to observe the crystal structure, monobasic lead sulfate, tribasic lead sulfate, which is in demand structure, and tetra basic lead sulfate. The SEM images are presented in Figure 4.22 and 4.23 (Wet mixes are at left column and dry mixes are at right column). The plates were prepared as it was mentioned at chapter 3. As it is seen from the figures that tribasic lead sulfate crystals, which are needle-like in shape and 3-5 μm length, was obtained as well as monobasic lead sulfate in small amount. This tribasic structure ensures that the paste has high specific active surface and strong mass structure as well as a good pore distribution for the paste.

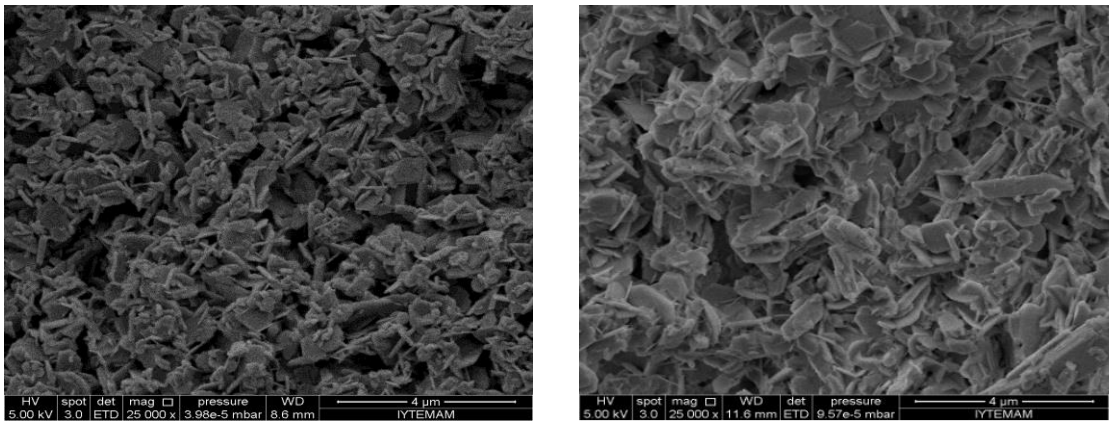

CB-1

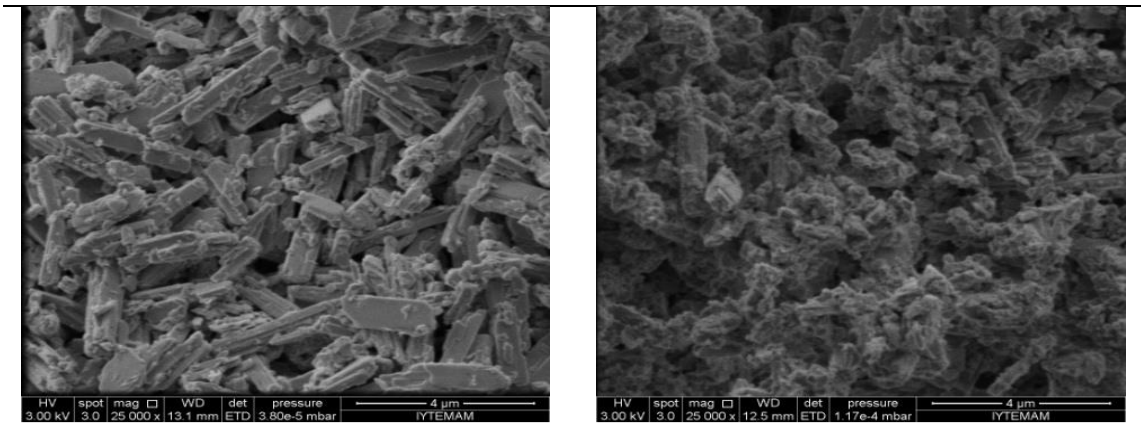

CB-2

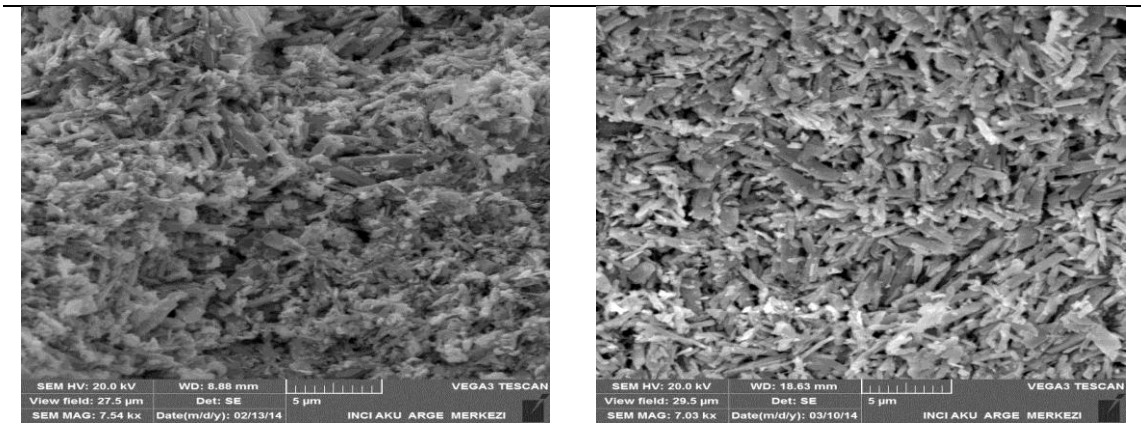

CB-3

Figure 4.22. SEM images of cured plates-1

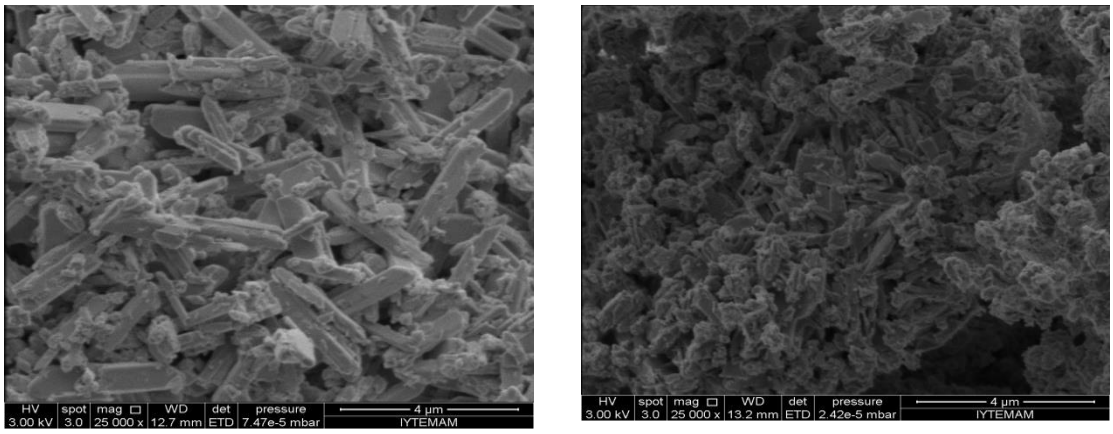

GR

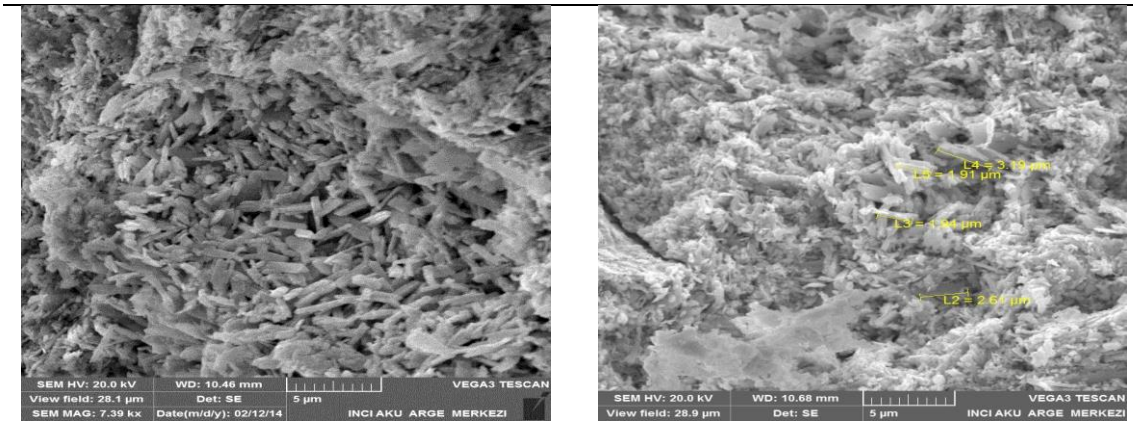

AC

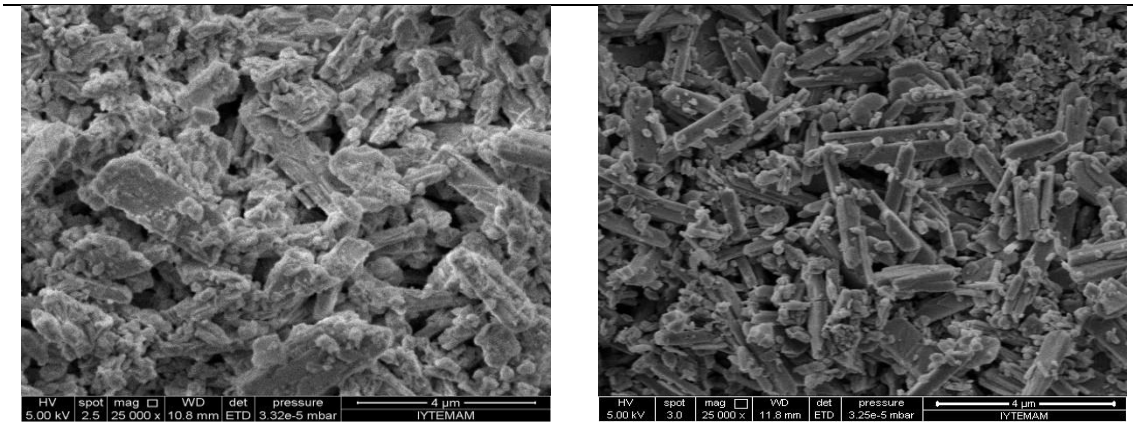

No Carbon

Figure 4.23. SEM images of cured plates-2.

4.3.2. X-ray Diffraction (XRD)

The X-ray diffraction patterns of cured negative plates are given in Figure 4.24 and 4.25, which belong to the wet mixes and dry mixes, respectively. A definitive list is given the following Table 4.1.

Table 4.1. Composition and 2θ values of crystals.

Nomenclature	Composition	2θ
A	$Pb_{10}(CO_3)_6O(OH)_6$	26.5
B	$3PbO.PbSO_4.H_2O$	27.4
C	$3PbO.PbSO_4.H_2O$, α-PbO, β-PbO	28.5, 28.62, 29.08
D	$3PbO.PbSO_4.H_2O$	31.0
E	$3PbO.PbSO_4.H_2O$, α-PbO	31.5 and 31.8
F	$3PbO.PbSO_4.H_2O$	32.9 and 33.2

The XRD patterns of $Pb_{10}(CO_3)_6O(OH)_6$, 3BS, α-PbO and β-PbO was observed, which was conformedby literature (Pavlov 2011a). The X-ray diffractogram plumbonacrite $Pb_{10}(CO_3)_6O(OH)_6$, which is shown by A, was formed as a result of interaction between $Pb(OH)_2$ from the paste and CO_2 from the air throughout curing process. β-PbO was observed at shoulder of region C. The formation of 3BS ensures the negative active material that has optimum pore distribution allowing way access of sulfuric acid ions and water molecules to each point of plate volume.

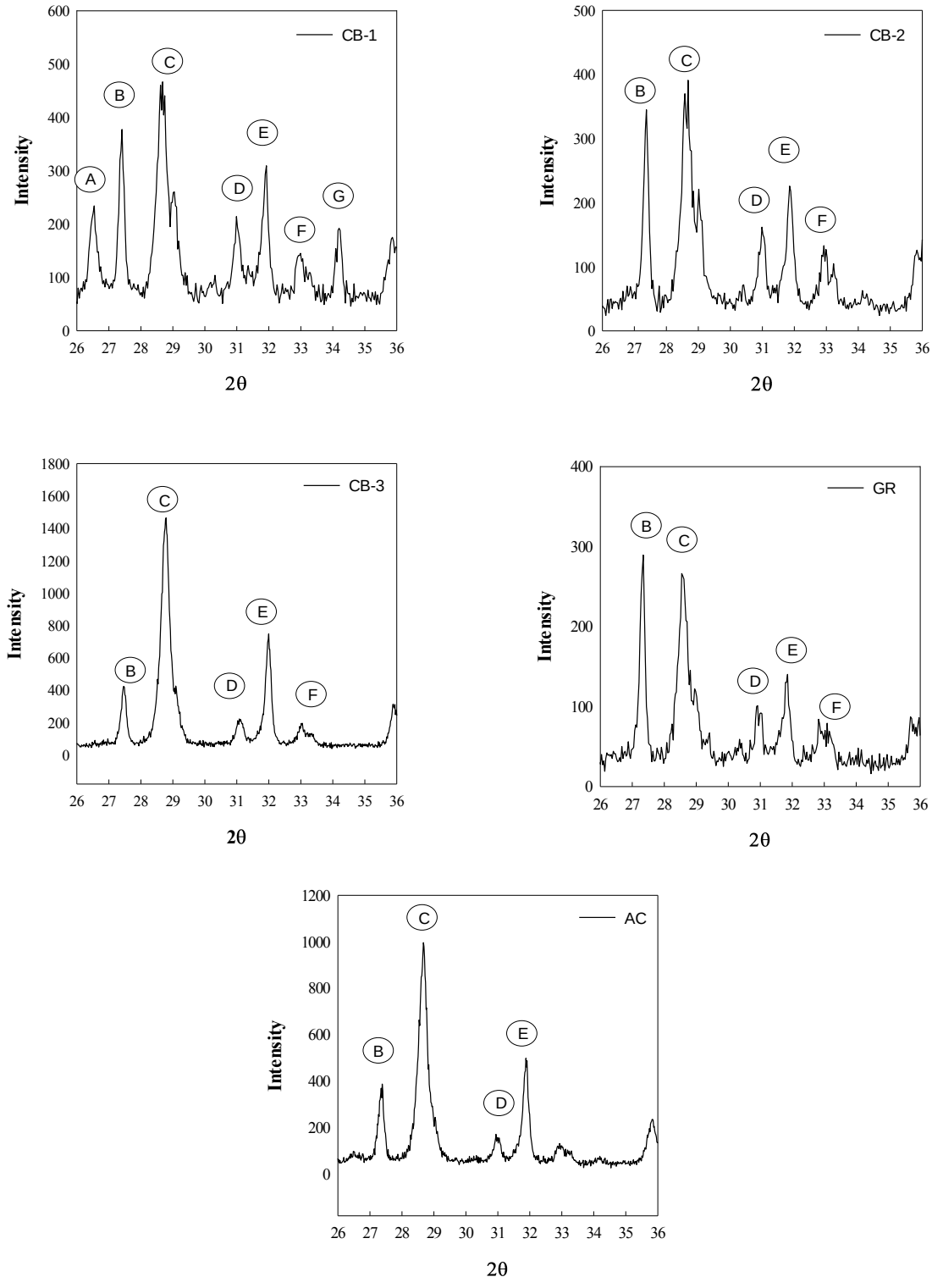

Figure 4.24. XRD patterns of cured plates prepared the method with wet mix

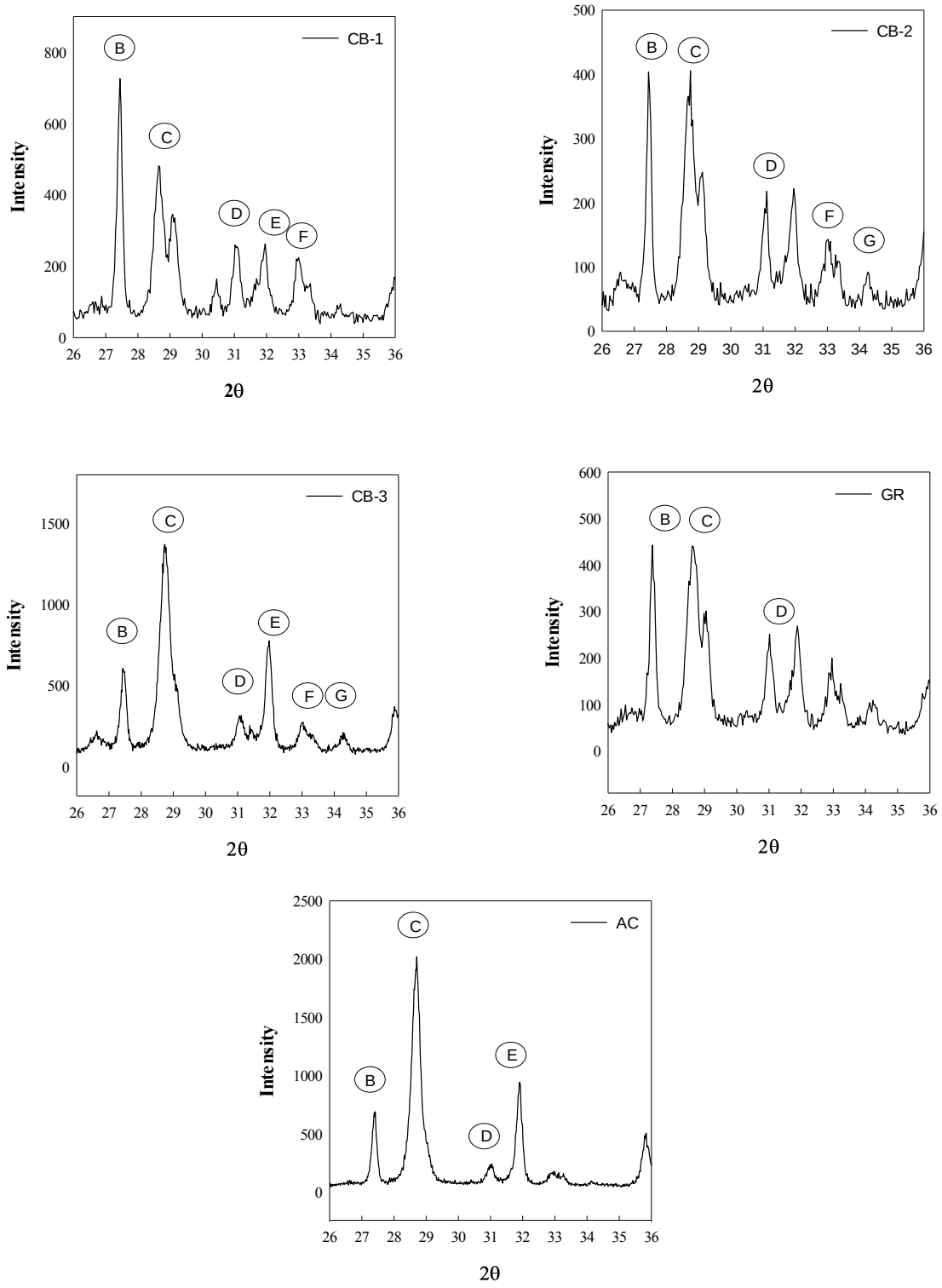

Figure 4.25. XRD patterns of cured plates prepared the method with dry mix

4.3.3. BET Surface Area

Surface area measurements of cured plates were determined by N_2 gas adsorption. The results are given in Table 4.2. The results show that there is no significant difference between the surface areas of the plates in terms of both the preparation method and the carbon type that they contain. The results are even similar in the case of no carbon case. This might be due to the dispersion problem of the carbons that has been discussed in the previous sections.

Table 4.2. Surface area of the plates.

Carbon	Surface Area (m^2/g)	
	Wet Mix	Dry Mix
CB-1	2.15	2.6
CB-2	2.27	2.85
CB-3	4.36	3.23
GR	3.25	2.89
AC	2.13	2.47

4.3.4.FT-IR Analysis

The FT-IR spectra of plates are given in Figure 4.26. The abbreviations 'wm' and 'dm' stand for wet mix and dry mix, respectively. The band at wavenumber 590 cm^{-1} can be attributed to vibrations of Pb-O metallic bond. The other bands at wavenumber 606, 960, 1030, 1090 and 1130 can be attributed to vibrations of $PbSO_4$ (Trettenhahn, Nauer, and Neckel 1996).

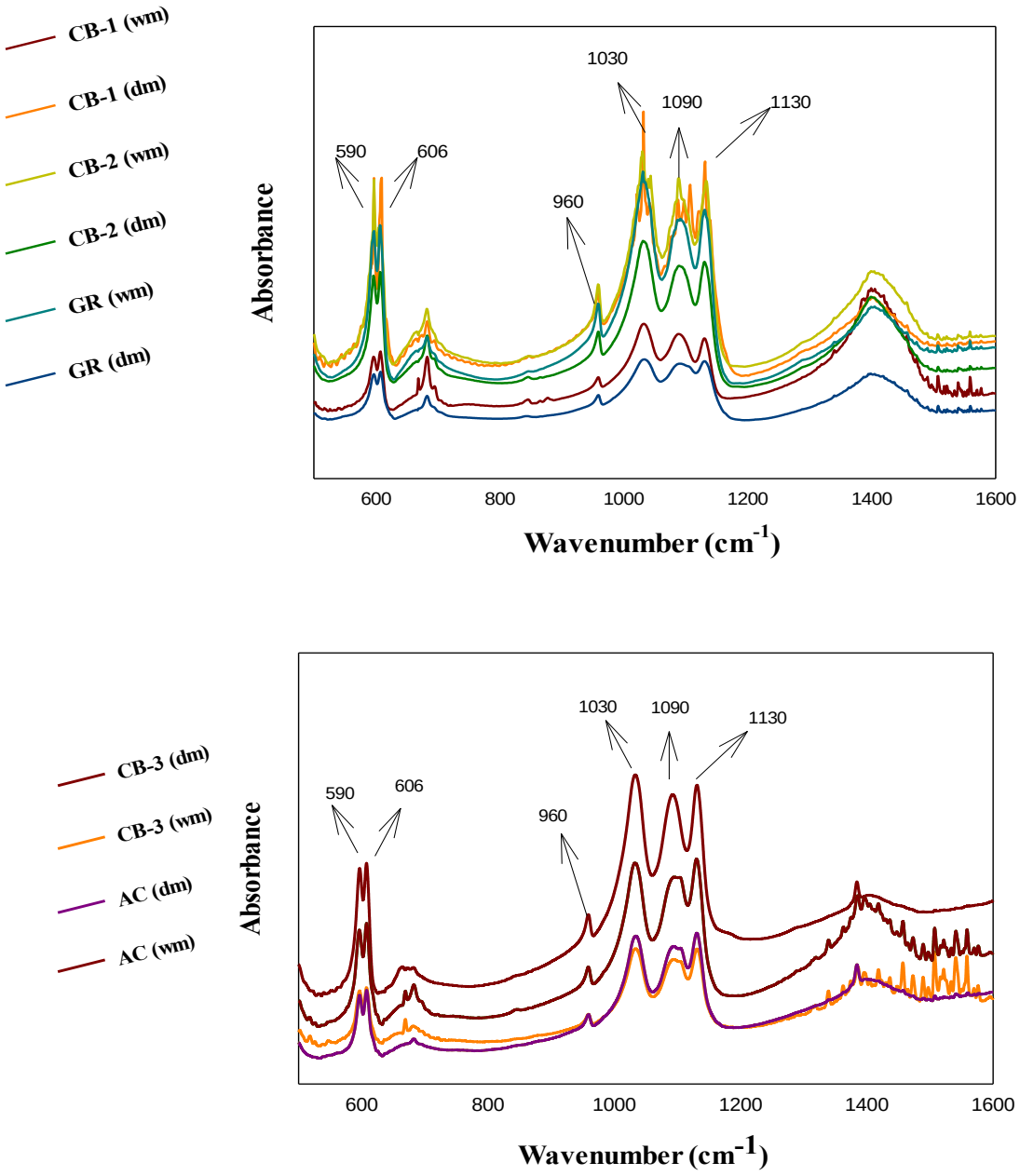

Figure 4.26. FT-IR spectras of plates.

4.3.5. Porosity Measurements

Porosity measurements of cured plates are performed and results given in Figure 4.27 and 4.28. The low porosity in the case of AC with very high surface area seems surprising at first glance. However, it is reasonable to expect that the overall porosity should not be affected by the porosity of the added carbon since the amount of carbon in the plate is very low (less than 0.1%). Therefore, an increase in the batch porosity by the

addition of very high surface area AC is negligible due to the very low addition amount of AC. Nevertheless, the size of the added carbon may have an important effect in the morphology of the plate. Remember that the size of the AC particles were very large (d50 around 30 micron) compared to other carbons with d50 values of around 3 to 5 microns (see Figures 4.10). That is other carbons are more comparable in size to the leady oxide with a d50 value of 3 microns (see Figures 4.3-4.9). It seems that very large AC particles affect the morphology of the plate since they are incompatible with the leady oxide particles and probably create a plate with less porosity.

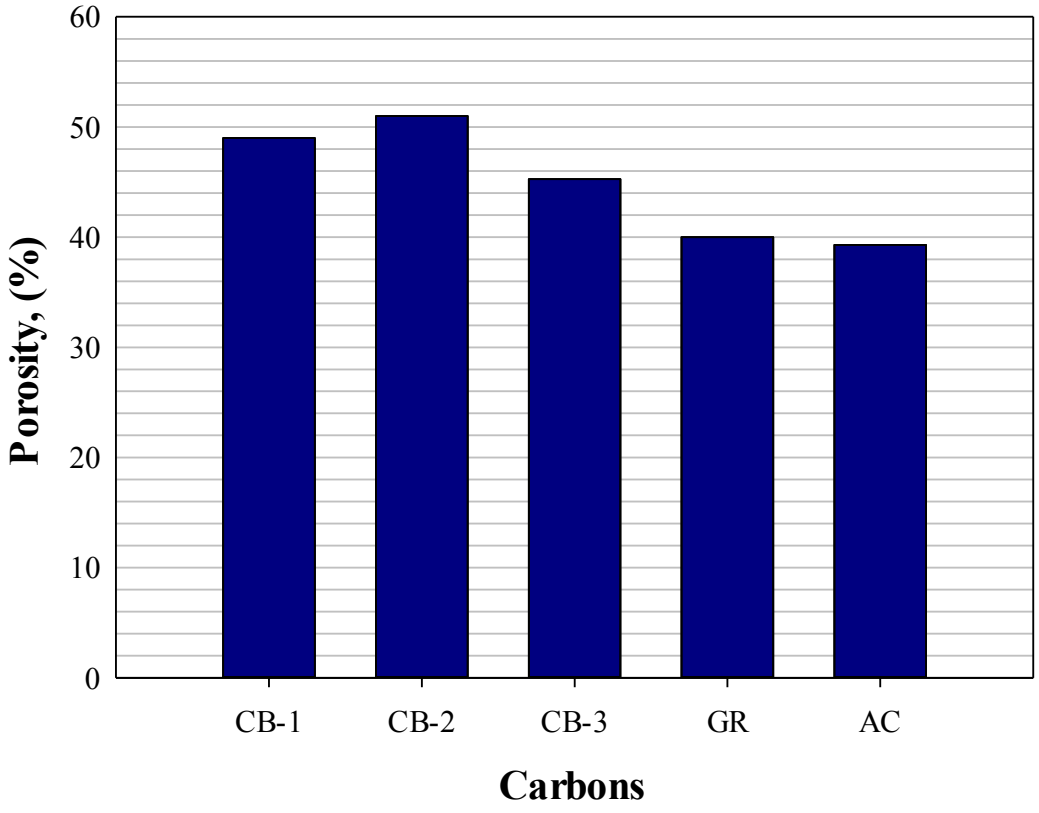

Figure 4.27. Porosity measurements of cured plates prepared the method with dry mix

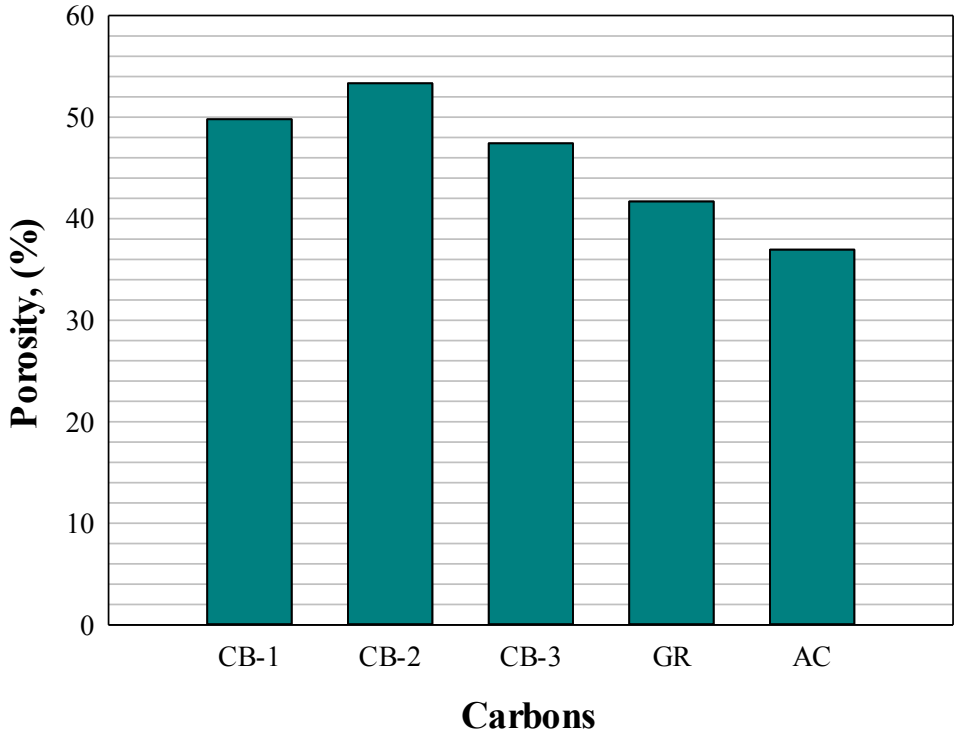

Figure 4.28. Porosity measurements of cured plates prepared the method with dry mix

4.4. Electrical Performance Tests of the Cured Negative Plates

Electrical performance, reserve capacity and cold-cranking ampere tests, was performed and the results are given in Table 4.4, and 4.5 for wet and dry mixtures, respectively. In addition to this, a cell from Battery Company production line was also charged to compare the test results that are given in Table 4.3.

In these tests the amount of carbon was kept constant and also mixing time of raw materials was increased. The results show that both the carbon type and the paste preparation method (dry or wet) have effects on the reserve capacity and cold-cranking ampere. In the case of wet mixing, the best result was obtained with carbon type CB-2 with 95 minutes of reverse capacity and 140 second of Cold-Cracking Ampere.

Table 4.3. Electrical performance result of reference cell

Carbon	Reserve Capacity (min)	CCA (sec)
CB-1	86	120

Table 4.4. Performance results of pastes prepared with dry mix method.

Carbon	Reserve Capacity (min)	CCA (sec)
CB-1	93	126
CB-2	91	126
CB-3	90	109
GR	78	95
AC	89	112

In the case of dry mixing, as seen in Table 4.4, the best result was obtained with CB-1 carbon mixture with 93 minutes of Reserve Capacity and 126 second of Cold-Cracking Ampere. These values are 86 minutes and 120 seconds in the case of Battery Company's plate. This shows that, in the case of dry mixing, increasing of mixing time of raw materials was affected performance results positively. In the case of wet mixing, as seen in Table 4.5, on the other hand, the results are better, the type of carbon seems to have some effect on the electrical performance of negative plates. But not as much as it is expected from it. So, the improvement in the mixing process (wet mixing) was not high enough to make carbon materials effective to increase the performance of plates. This is most probably due to the dispersing problems of the carbon materials being used in making negative paste plates. Industries should seek a suitable carbon material for this purpose so that they can increase the electrical performance of their batteries.

Table 4.5. Performance results of pastes prepared with wet mix method.

Carbon	Reserve Capacity (min)	CCA (sec)
CB-1	96	134
CB-2	95	140
CB-3	91	104
GR	74	90
AC	89	98

4.4.1. The Effect of Amount of Barium Sulfate and Lignosulfonate

The effect of other ingredients such as barium sulfate and lignosulfonate were also tested and the results are given in Table 4.6 and 4.7, respectively. In the studies with $BaSO_4$, A, B and C stand for the amount of $BaSO_4$ used, 2, 2.5 and 3-fold respectively. In the studies with lignosulfonate, D, E and F stand for the amount of lignosulfonate used, 1.4, 1.7 and 2-fold respectively. As it is seen from these results that the highest reserve capacity result with 98 minutes has been reached when the amount of $BaSO_4$ was increased by 2-folt of its normal amount.

A paste that has no lignosulfonate was also prepared and cured to observe the behavior of negative past. Other additives and components were kept constant during this experiment. Scale bars of SEM images are 20 and 5μm, were given in Figure 4.33. The length of three crystals was randomly measured with the program in device as 4.43, 4.58 and 4.65μm. These results are attributed to that using lignosulfonate in negative electrode makes difficult the formation of 3BS crystals. Moreover this plate was charged then SEM image of negative active material (spongy lead) was taken and given Figure 4.33 in two different scale bars, 20 and 10μm. Also a negative material which includes lignosulfonate are given in Figure 4.34 to compare the result (Saravanan, Ganesan, and Ambalavanan 2014).

Table 4.6. Performance results of studies performed with $BaSO_4$.

Percent of $BaSO_4$	**Reserve Capacity(min)**	**CCA(sec)**
% A	88	97
% B	98	118
% C	90	113

As it is seen from Figure 4.33 that in the absence of lignosulfonate, the very nicely crystallized tribasic structures formed. However, it seems that the addition of lignosulfonate affect the behavior of the paste negatively during charging more than anything else. The figures show that in the absence of lignosulfonate, the perfectly formed tribasic crystals somehow coalesce and form formed tribasic crystals somehow coalesce and form much larger structures which are not favorable in terms of capacity.

Table 4.7. Performance results of studies performed with lignosulfonate.

Percent of Lignosulfonate	Reserve Capacity (min)	CCA (sec)
% D	82	110
% E	84	112
% F	82	117

. This is also in agreement with the literature which states that in the absence of lignosulfonate the capacity of the active material is lowered (Pavlov, Nikolov, and Rogachev 2010a) .

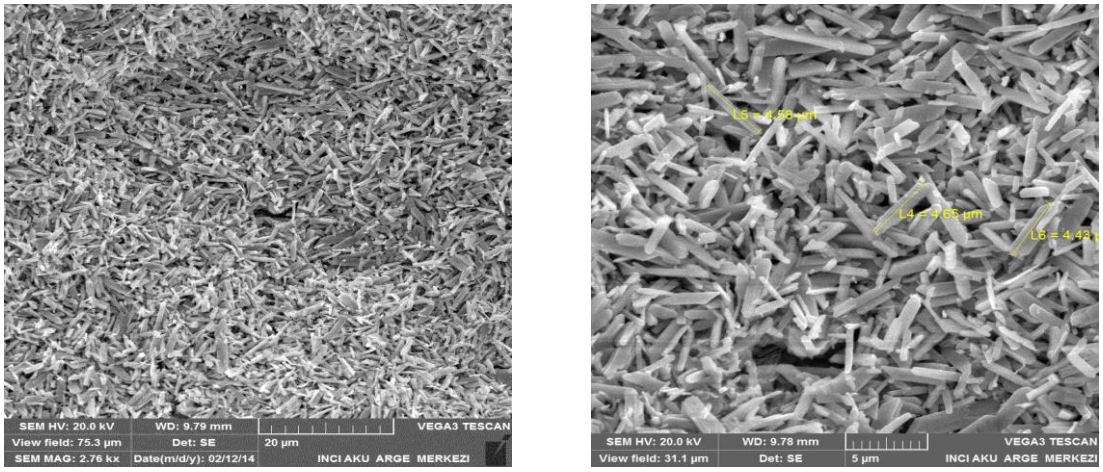

Figure 4.29. SEM images of the paste without lignosulfonate

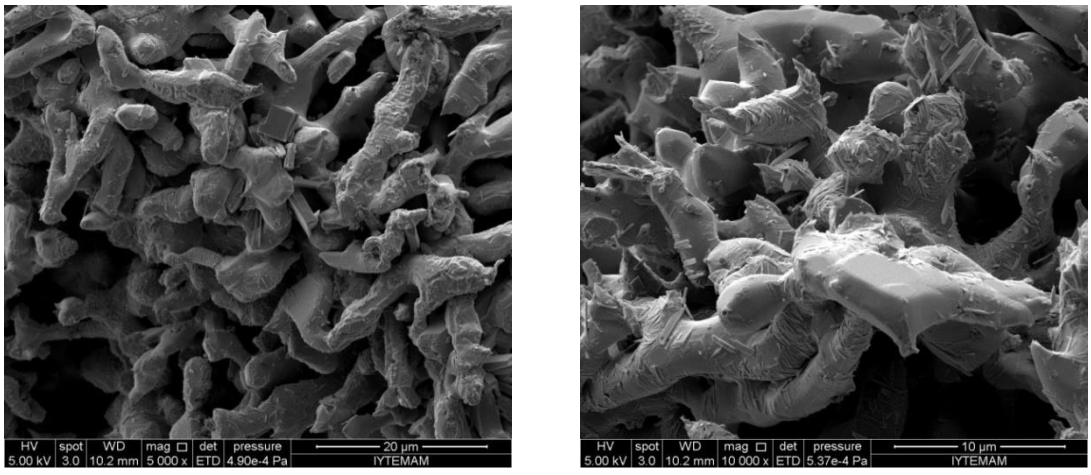

Figure 4.30. SEM image of the negative active material without lignosulfonate

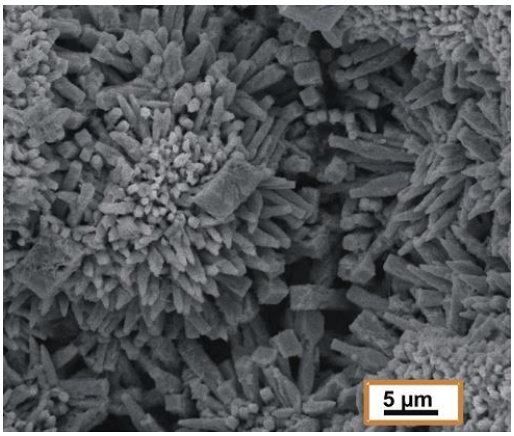

Figure 4.31. SEM image of negative active material with lignosulfonate.

4.5. Prototype Battery Production and Performance Results

Using the results of this study, prototype batteries were produced and electrical performance tests, reserve capacity, cold-cranking ampere and cycling were performed. These results are given in Table 4.9 and 4.10. The plates prepared with %B $BaSO_4$ had the highest reserve capacity among all plates and a good CCA. Hence, the percent of barium sulfate was taken as % B the following recipes of prototype batteries.

In Table 4.8, the values in standard column represent the battery capacity and CCA, which are the minimum values before beginning cycle life test. For this purpose, firstly the plates produced for prototype batteries were checked with forming a cell and charged to observe whether they have required minimum capacity and CCA. Negative paste of first prototype battery was prepared with CB-1 carbon and %B $BaSO_4$, while second one was prepared with CB-2 carbon and %B $BaSO_4$ by wet mix method. The amount of carbons was the same with company. The reason to choose the CB-1 and CB-2 was the particle size distribution of them compare with others. Even though they weren't shown great particle size distribution they had the best reserve capacity and CCA results when plates were charged (Section 4.4). As it is seen from Table 4.8., plates shown the 76.16 and 78.26 Ah capacities and 178 and 181 second CCA values, which are above required reserve capacity and CCA. After that plates were assembled and then batteries were charged.

The results, in Table 4.9 and 4.10, show that batteries reached and passed the 36000 cycle number, which is minimum number for a micro-hybrid vehicle. Moreover,

batteries had CCA value, which is higher than minimum value 60 second. Besides this, capacity values were over the minimum value. These results were attributed to changes when the paste was prepared. Firstly, the mixing time of raw materials, which was performed for 4 minutes, was increased to 10 min to obtain more homogenous mixing. Secondly, wet mix method is used to improve the dispersibility of carbon. Thus, it may increase the effectiveness of carbon. Thirdly this improvement was related with effect of increasing amount of barium sulfate. It can be attributed that $BaSO_4$ ensures the uniform distribution of lead sulfates ($PbSO_4$) and retard forming of unsoluble $PbSO_4$ crystals, which cause the battery failure.

Table 4.8. The properties of prototype batteries

PROTOTYPE BATTERIES			
Number of Prototype Battery		**1st**	**2nd**
Standard	**Capacity(Ah)**	72	72
	CCA(Ampere)	600	600
	CCA(second)	140	140
Experiment	**Capacity(Ah)**	76,16 Ah	78,26 Ah
	% Capacity Success	106	109
	CCA(second) (>140 sec)	178	181
	Result	**Successful**	**Successful**

Table 4.9. The results of first prototype battery

1st Battery			
Cycle Number	12000	24000	36000
Capacity (Ah)	76,16	76,16	76,16
Final Reserve Capacity	70,12	61,4	59,2
Percent of Capacity (%)	92	80	78
Terminal Voltage (V) (>7 V)	7,86	7,77	7,42
CCA (second)(> 60s)	137	103	83
Result	**Successful**	**Successful**	**Successful**

Table 4.10. The results of second prototype battery

2nd Battery			
Cycle Number	12000	24000	36000
Capacity (Ah)	78,26	78,26	78,26
Final Reserve Capacity	70,9	61,9	53,8
Percent of Capacity (%)	90	79	69
Terminal Voltage (V) (>7 V)	7,9	7,71	7,59
CCA (second)(> 60s)	146	92	76
Result	**Successful**	**Successful**	**Successful**

CHAPTER 5

CONCLUSIONS

Lead-acid batteries that are necessary as electrochemical power source for automotives suffer from sulfation of negative electrode inevitably. Additives used in negative electrode not suppress the sulfation of the plates completely but prolong battery's life.

However, there is no exact and confidential information in literature about how the additives work and affect the negative active material.

In this study, it was aimed to improve the commercial lead-acid battery for micro- hybrid (start-stop) vehicles and elucidate the exact working mechanism of lead-acid battery negative active material. For this purpose, experimental studies were conducted in three parts. First one is the characterizing of negative active material raw materials, leady oxide, lignosulfonate, carbon, barium sulfate. These are size and charge measurements of leady oxide, carbon and barium sulfate in distilled water and lignosulfonate solutions, surface tension measurements with lignin sulfonate solutions. Second one is determination of rheological properties of negative paste in different cases. Third one is the performance testes of negative plates prepared from the pastes characterized results from other parts. The performance tests conducted were reserve capacity, cold-cranking ampere (CCA) and cycle life measurements.

In the first part of studies, it was shown that the all of carbon materials suffer from agglomeration in water and lignosulfonate solutions which were prepared in different concentrations. The average size of leady oxide particles increased after a critical concentration (5x10-3 M) of lignosulfonate. The charge of leady oxide surface was positive in the absence of lignosulfonate in water and changed to negative with increasing concentration of lignosulfonate. In the second part of the study, the rheological properties of negative paste were determined in different preparation cases and shown that the amount of additives and preparation method has big effects. In the third part of the study, the negative plates were prepared with two methods, wet and dry mixing and then electrical tests such as reserve capacity, CCA and cycle life

measurements were performed. It was found that type of carbon materials does not contribute to reserve capacity but affect CCA.

Based on the results of this study, the following specific conclusions can be made:

- Wet Mixing Method was employed to improve dispersion of carbon in NAM. It was seen that this method also;
  - ❖ affected paste viscosity positively
  - ❖ resulted in more pronounced tri-basic lead sulfate crystals
  - ❖ enhanced paste surface areas
  - ❖ improved the porosity slightly
- The prototype cells formed from the NAM prepared with the Wet Mixing Method yielded increased reserve capacity and CCA values compared with the company recipe.
- Two prototype batteries formed from the NAM prepared with the Wet Mixing Method exceed the requirements of battery standards for Micro Hybrid Battery cycling tests.
- An optimum amount of $BaSO_4$ was also found to be important in the performance of a battery.

REFERENCES

1966. "Burbank and Wales to Receive Battery Division Research Award for 1966–1967." *Journal of The Electrochemical Society* 113 (9):247C. doi: 10.1149/1.2424142.

Aidman, G. I. 1996. "A view on chemically synthesized expanders for lead/acid battery negative plates." *Journal of Power Sources* 59 (1–2):25-30. doi: http://dx.doi.org/10.1016/0378-7753(95)02297-X.

Asai, Kenji, Masaharu Tsubota, Kunio Yonezu, and Koji Ando. 1981. "Discharge behaviour of electrodeposited PbO2 and Pb electrodes." *Journal of Power Sources* 7 (1):83-94. doi: http://dx.doi.org/10.1016/0378-7753(81)80061-4

Ban, I., Y. Yamaguchi, Y. Nakayama, N. Hirai, and S. Hara. 2002. "In situ EC-AFM study of effect of lignin on performance of negative electrodes in lead−acid batteries." *Journal of Power Sources* 107 (2):167-172. doi: http://dx.doi.org/10.1016/S0378-7753(01)01002-3.

Biagetti, R. V., and M. C. Weeks. 1970. "TETRABASIC LEAD SULFATE AS A PASTE MATERIAL FOR POSITIVE PLATES." *Bell System Technical Journal* 49 (7):1305.

Blair, T. L. 1998. "Lead oxide technology—Past, present, and future." *Journal of Power Sources* 73 (1):47-55. doi: http://dx.doi.org/10.1016/S0378-7753(97)02781-X.

Boden, D. P. 1998. "Selection of pre-blended expanders for optimum lead/acid battery performance." *Journal of Power Sources* 73 (1):89-92. doi: http://dx.doi.org/10.1016/S0378-7753(98)00026-3.

Boden, D. P. 2004. "Comparison of methods for adding expander to lead-acid battery plates—advantages and disadvantages." *Journal of Power Sources* 133 (1):47-51. doi: http://dx.doi.org/10.1016/j.jpowsour.2003.12.006.

Boden, D. P., D. V. Loosemore, M. A. Spence, and T. D. Wojcinski. 2010. "Optimization studies of carbon additives to negative active material for the purpose of extending the life of VRLA batteries in high-rate partial-state-of-charge operation." *Journal of Power Sources* 195 (14):4470-4493. doi: http://dx.doi.org/10.1016/j.jpowsour.2009.12.069.

Catherino, Henry A., Fred F. Feres, and Francisco Trinidad. 2004. "Sulfation in lead–acid batteries." *Journal of Power Sources* 129 (1):113-120. doi: http://dx.doi.org/10.1016/j.jpowsour.2003.11.003.

Ekdunge, P., and D. Simonsson. 1989. "The discharge behaviour of the porous lead electrode in the lead-acid battery. I. Experimental investigations." *Journal of Applied Electrochemistry* 19 (2):127-135. doi: 10.1007/BF01062289.

Hampson, N. A., J. B. Lakeman, K. S. Sodhi, and J. G. Smith. 1980. "The effect of additives on the charge and discharge behaviour of the negative plate of the lead-acid battery." *Surface Technology* 11 (5):377-384. doi: http://dx.doi.org/10.1016/0376-4583(80)90055-2.

Hirai, N., D. Tabayashi, M. Shiota, and T. Tanaka. 2004. "In situ electrochemical atomic force microscopy of lead electrodes in sulfuric acid solution with or without lignin during anodic oxidation and cathodic reduction." *Journal of Power Sources* 133 (1):32-38. doi: http://dx.doi.org/10.1016/j.jpowsour.2003.12.020.

Iliev, V., and D. Pavlov. 1979. "INFLUENCE OF PBO MODIFICATION ON THE KINETICS OF THE 4PBO.PBSO4 LEAD-ACID-BATTERY PASTE FORMATION." *Journal of Applied Electrochemistry* 9 (5):555-562. doi: 10.1007/bf00610941.

Moseley, P. T., R. F. Nelson, and A. F. Hollenkamp. 2006. "The role of carbon in valve-regulated lead–acid battery technology." *Journal of Power Sources* 157 (1):3-10. doi: http://dx.doi.org/10.1016/j.jpowsour.2006.02.031.

Moseley, P. T., and D. A. J. Rand. 2004. "Chapter 1 - The Valve-regulated Battery — A Paradigm Shift in Lead-Acid Technology." In *Valve-Regulated Lead-Acid Batteries*, edited by D. A. J. RandJ GarcheP T. MoseleyC D. Parker, 1-14. Amsterdam: Elsevier.

Myrvold, Bernt O. 2003. "Interactions between lignosulphonates and the components of the lead-acid battery: Part 1. Adsorption isotherms." *Journal of Power Sources* 117 (1–2):187-202. doi: http://dx.doi.org/10.1016/S0378-7753(03)00018-1.

Nakamura, K., M. Shiomi, K. Takahashi, and M. Tsubota. 1996. "Failure modes of valve-regulated lead/acid batteries." *Journal of Power Sources* 59 (1–2):153-157. doi: http://dx.doi.org/10.1016/0378-7753(95)02317-8.

Papazov, G. 2009. "SECONDARY BATTERIES – LEAD– ACID SYSTEMS | Negative Electrode." In *Encyclopedia of Electrochemical Power Sources*, edited by Jürgen Garche, 576-589. Amsterdam: Elsevier.

Pavlov, D. 1992. "The Lead-Acid Battery Lead Dioxide Active Mass: A Gel-Crystal System with Proton and Electron Conductivity." *Journal of The Electrochemical Society* 139 (11):3075-3080. doi: 10.1149/1.2069034.

Pavlov, D., and P. Nikolov. 2013. "Capacitive carbon and electrochemical lead electrode systems at the negative plates of lead–acid batteries and elementary processes on cycling." *Journal of Power Sources* 242 (0):380-399. doi: http://dx.doi.org/10.1016/j.jpowsour.2013.05.065.

Pavlov, D., P. Nikolov, and T. Rogachev. 2010a. "Influence of expander components on the processes at the negative plates of lead-acid cells on high-rate partial-state-of-charge cycling. Part I: Effect of lignosulfonates and BaSO4 on the processes of charge and discharge of negative plates." *Journal of Power Sources* 195 (14):4435-4443. doi: http://dx.doi.org/10.1016/j.jpowsour.2009.11.060.

Pavlov, D., P. Nikolov, and T. Rogachev. 2010b. "Influence of expander components on the processes at the negative plates of lead-acid cells on high-rate partial-state-of-charge cycling. Part II. Effect of carbon additives on the processes of charge and discharge of negative plates." *Journal of Power Sources* 195 (14):4444-4457. doi: http://dx.doi.org/10.1016/j.jpowsour.2009.12.132.

Pavlov, D., P. Nikolov, and T. Rogachev. 2011. "Influence of carbons on the structure of the negative active material of lead-acid batteries and on battery performance." *Journal of Power Sources* 196 (11):5155-5167. doi: http://dx.doi.org/10.1016/j.jpowsour.2011.02.014.

Pavlov, D., and G. Papazov. 1976. "DEPENDENCE OF PROPERTIES OF LEAD-ACID-BATTERY POSITIVE PLATE PASTE ON PROCESSES OCCURRING DURING ITS PRODUCTION." *Journal of Applied Electrochemistry* 6 (4):339-345. doi: 10.1007/bf00608919.

Pavlov, Detchko. 2011a. "Chapter 1 - Invention and Development of the Lead–Acid Battery." In *Lead-Acid Batteries: Science and Technology*, edited by Detchko Pavlov, 3-28. Amsterdam: Elsevier.

Pavlov, Detchko. 2011b. "Chapter 2 - Fundamentals of Lead–Acid Batteries." In *Lead-Acid Batteries: Science and Technology*, edited by Detchko Pavlov, 29-114. Amsterdam: Elsevier.

Pavlov, Detchko. 2011c. "Chapter 3 - H2SO4 Electrolyte – An Active Material in the Lead–Acid Cell." In *Lead-Acid Batteries: Science and Technology*, edited by Detchko Pavlov, 117-148. Amsterdam: Elsevier.

Pavlov, Detchko. 2011d. "Chapter 5 - Leady Oxide." In *Lead-Acid Batteries: Science and Technology*, edited by Detchko Pavlov, 223-250. Amsterdam: Elsevier.

Pavlov, Detchko. 2011e. "Chapter 6 - Pastes and Grid Pasting." In *Lead-Acid Batteries: Science and Technology*, edited by Detchko Pavlov, 253-309. Amsterdam: Elsevier.

Pavlov, Detchko. 2011f. "Chapter 7 - Additives to the Pastes for Positive and Negative Battery Plates." In *Lead-Acid Batteries: Science and Technology*, edited by Detchko Pavlov, 311-361. Amsterdam: Elsevier.

Pavlov, Detchko. 2011g. "Chapter 8 - Curing of Battery Plates." In *Lead-Acid Batteries: Science and Technology*, edited by Detchko Pavlov, 363-404. Amsterdam: Elsevier.

Pavlov, Detchko. 2011h. "Chapter 11 - Processes During Formation of Negative Battery Plates." In *Lead-Acid Batteries: Science and Technology*, edited by Detchko Pavlov, 481-499. Amsterdam: Elsevier.

Rand, D. A. J., and P. T. Moseley. 2009. "SECONDARY BATTERIES – LEAD–ACID SYSTEMS | Overview." In *Encyclopedia of Electrochemical Power Sources*, edited by Jürgen Garche, 550-575. Amsterdam: Elsevier.

Ruetschi, Paul. 2004. "Aging mechanisms and service life of lead–acid batteries." *Journal of Power Sources* 127 (1–2):33-44. doi: http://dx.doi.org/10.1016/j.jpowsour.2003.09.052.

Saravanan, M., M. Ganesan, and S. Ambalavanan. 2014. "An in situ generated carbon as integrated conductive additive for hierarchical negative plate of lead-acid battery." *Journal of Power Sources* 251 (0):20-29. doi: http://dx.doi.org/10.1016/j.jpowsour.2013.10.143.

Sawai, Ken, Takayuki Funato, Masashi Watanabe, Hidetoshi Wada, Kenji Nakamura, Masaaki Shiomi, and Shigeharu Osumi. 2006. "Development of additives in negative active-material to suppress sulfation during high-rate partial-state-of-charge operation of lead–acid batteries." *Journal of Power Sources* 158 (2):1084-1090. doi: http://dx.doi.org/10.1016/j.jpowsour.2006.01.096.

Shiomi, Masaaki, Takayuki Funato, Kenji Nakamura, Katsuhiro Takahashi, and Masaharu Tsubota. 1997. "Effects of carbon in negative plates on cycle-life performance of valve-regulated lead/acid batteries." *Journal of Power Sources* 64 (1–2):147-152. doi: http://dx.doi.org/10.1016/S0378-7753(96)02515-3.

Trettenhahn, G. L. J., G. E. Nauer, and A. Neckel. 1996. "In situ external reflection absorption FTIR spectroscopy on lead electrodes in sulfuric acid." *Electrochimica Acta* 41 (9):1435-1441. doi: http://dx.doi.org/10.1016/0013-4686(95)00389-4.

Vallat-Joliveau, F., A. Delahaye-Vidal, M. Figlarz, and A. de Guibert. 1995. "Some Structural and Textural Aspects of Tribasic Lead Sulfate Precipitation during the Mixing of Lead-Acid Battery Positive Paste." *Journal of The Electrochemical Society* 142 (8):2710-2716. doi: 10.1149/1.2050079.

Vermesan, H., N. Hirai, M. Shiota, and T. Tanaka. 2004. "Effect of barium sulfate and strontium sulfate on charging and discharging of the negative electrode in a lead–acid battery." *Journal of Power Sources* 133 (1):52-58. doi: http://dx.doi.org/10.1016/j.jpowsour.2003.11.071.

Wagner, R. 2009. "SECONDARY BATTERIES – LEAD– ACID SYSTEMS | Curing and Formation." In *Encyclopedia of Electrochemical Power Sources*, edited by Jürgen Garche, 662-676. Amsterdam: Elsevier.

Xiang, Jiayuan, Ping Ding, Hao Zhang, Xianzhang Wu, Jian Chen, and Yusheng Yang. 2013. "Beneficial effects of activated carbon additives on the performance of negative lead-acid battery electrode for high-rate partial-state-of-charge operation." *Journal of Power Sources* 241 (0):150-158. doi: http://dx.doi.org/10.1016/j.jpowsour.2013.04.106.